MISSOURI
S&T
Library and
Learning Resources

Scholars' Mine

Doctoral Dissertations   Student Theses and Dissertations

Summer 2015

Application of unified invariants for cyber physical systems in smart grids

Tamal Paul

Follow this and additional works at: https://scholarsmine.mst.edu/doctoral_dissertations

Part of the Electrical and Computer Engineering Commons

Department: Electrical and Computer Engineering

APPLICATION OF UNIFIED INVARIANTS FOR CYBER PHYSICAL SYSTEMS IN

SMART GRIDS

by

TAMAL PAUL

A DISSERTATION

Presented to the Graduate Faculty of the

MISSOURI UNIVERSITY OF SCIENCE AND TECHNOLOGY

In Partial Fulfillment of the Requirements for the Degree

DOCTOR OF PHILOSOPHY

in

ELECTRICAL ENGINEERING

2015

Approved by

Dr. Jonathan Kimball, Advisor
Dr. Mariesa Crow
Dr. Maciej Zawodniok
Dr. Sriram Chellappan
Dr. Bruce McMillin

PUBLICATION DISSERTATION OPTION

This dissertation has been prepared in the form of three papers. Pages 9–27 has been submitted as *Distributed Grid Intelligence integrated Invariant Based Method for analyzing Voltage Stability in Smart-Grids*, IEEE Transactions on Smart Grid (2015) with Tamal Paul, Thomas P. Roth, Bruce McMillin, Harsha Ravindra, Michael Steurer, and Jonathan W. Kimball. Pages 28–45 will be submitted as *Distributed Grid Intelligence enabled Line Flow Invariants for Transaction based Smart-Grids*, IEEE Transactions on Smart Grid (2015), Tamal Paul, Thomas P. Roth, Bruce McMillin, Harsha Ravindra, Michael Steurer, and Jonathan W. Kimball. Pages 46–60 will be submitted as *Transient Stability Monitoring Invariants in Microgrids*, IEEE Transactions on Control Systems Technology (2015), with Tamal Paul, Md. Rasheduzzaman, and Jonathan W. Kimball.

ABSTRACT

Cyber-Physical Systems (CPS) are complex engineered systems which consist of physical components with an underlying cyber network. The three main components of a cyber-physical System are: physical system, networking and communications element and a distributed cyber system. The primary challenge for cyber-physical systems is to understand what happens when various sub-systems, which have been developed in an isolated environment, are integrated. CPS studies need to ensure sub-systems that had been designed in isolation to meet certain specifications, when combined, do not cause the overall system to fail. The crux of cyber-physical research is thus to find a common platform to bind all these different components, so as to monitor the overall system performance.

This dissertation discusses how to unify these different aspects and tackles the issue of synthesizing, verifying and monitoring highly diverse environments by introducing the concept of Unified Invariants. In this dissertation, a smart grid has been used to implement and validate this concept of Unified Invariants towards building a robust cyber-physical system. There are several ways to compromise the reliable operation of a smart grid. Examples of such contingent events are voltage collapse, line overloading and transient stability. Physical system invariants have been developed to identify and thwart such events which threaten the integrity of the physical system. These physical invariants have be integrated with cyber controllers to ensure a safe, stable and reliable operation of the smart grid. This is an unique concept and differs from previous methods in the fact that while earlier methods have tried to compose functionality of each domain of the cyber-physical world, the Unified Invariant method serves as a transformative approach to express and impose system properties that are common to all the domains (cyber, physical, networking). The net outcome of such an approach is that the resulting CPSs will be safe and stable at the system level, rather than just the sub-system level.

ACKNOWLEDGMENTS

TABLE OF CONTENTS

SECTION

LIST OF ILLUSTRATIONS

PAPER III

LIST OF TABLES

SECTION

1. INTRODUCTION

1.1. UNIFIED INVARIANTS IN MULTI DOMAIN CYBER-PHYSICAL SYSTEMS

Cyber-physical systems are multi disciplinary systems, which means they are comprised of different sub-systems using distinct metrics and methods. The foundational approach of this research is fundamentally different from any other kind of CPS work because the focus here is to compose such different sub-systems, not through their functionality but through their correctness to create safe, stable and predictable multi disciplinary systems. Thus, we construct CPSs through compositional integration of the cyber, networking, scheduling, and physical components rooted in correctness. Examples of such systems include the electrical smart grid, unmanned air vehicles and automated motor vehicles on the highway. The common underlying feature of all these systems is that not only do they have complicated physical dynamics (physical systems) governing them, but also relatively complex distributed computation (cyber systems) and communication (network systems). This gives rise to the fundamental question of how to compose such correct multi disciplinary systems.

When treated in isolation, it is diifficult to grasp why certain constraints are present in a system; for instance, why is there a certain maximum message delay or why does a certain scheduling deadline needs to be met? These questions can only be partially answered by developing individual invariants; the response of the entire CPS is based on the composition of these invariants. Thus, the concept of unified invariants makes it possible to develop an approach to compositionally integrate the CPS system aspects. In each aspect, cyber, physical, scheduling and network, stability invariants, based on individual

system theories are developed. These invariants are refined through the property of noninterference to develop a CPS. The first step in the application of Unified Invariants to study cyber-physical systems is to create predictable multi disciplinary systems by composing the distinct sub-systems not through their mere functionality but also through their correctness.

"Invariant", as used here is a common terminology in the cyber domain. An invariant is a logical predicate on a system state that must remain true throughout system execution [1]. However, every domain has its own way of denoting correctness. The fundamental challenge in this case is how to make all the domains speak in the same language. Unified Invariants serve as the lingua franca for all sub-systems of a CPS.

Invariants, although well known in the cyber world are not much used in other domains. But every domain has its own equivalent of invariants to define correctness and the challenge is to translate the language of each of these domains to the lingua franca of invariants. The following sections give a few initial translations for the domains of interest.

1.1.1. Physical Systems. The physical system specifications can be broadly divided into constraints. There can be various constraints to monitor the correctness of a physical system. Example constraints include maximum or minimum voltage at a certain bus in a smart grid, the amount of power that can flow in a line in the power system, transient stability and frequency stability. These constraints serve as the physical system equivalent of invariants. These constraints can be expressed as in equality/inequality whose truth value denotes the invariant. In other words, if the constraint is satisfied, the invariant is true and system correctness is maintained. If the constraint is not satisfied, the invariant is false and system correctness is no longer preserved.

1.1.2. Networks. The network correctness is quantified by means of desired reliability in delivery of packets and the desired quality of service. (QoS). The metrics include minimum throughput, minimum packet delivery ratio, maximum delay and maximum jitter. The network correctness is hampered by various interference vectors including increased traffic generation, link failures and external RF interference. As the controller requests

increase, the network congestion increases which leads to delay in transferring packets thereby causing lower throughput and eventually results in packet losses. Consequently the invariant fails thereby potentially affecting the CPS's overall correctness.

1.1.3. Scheduling. In traditional real time embedded systems, correct scheduling refers to deterministic scheduling with a priori schedulability guarantees [2]. In a networked or distributed real-time embedded system, scheduling frameworks on each component typically abstract the details of the network in the form of bounded delays. However the intricately dynamic nature of the physical system and complex distributed operations makes such kind of scheduling unrealistic for CPSs. This is due to the fact that delays and system stability in a CPS are not only contingent to system design but also on changes in the physical environment, cyber failure and recovery, lost packets, congestion, changes in topology and complex distributed computations and optimizations. Moreover, in a cyber-physical system, the actions of one domain may affect other domains. Such inter-domain actions need to be scheduled properly. Therefore in light of all these changes, it is very important to develop a scheduling that can adapt its behavior in response to system state and hence the need for adaptive scheduling arises.

It is quite natural to express Adaptive scheduling as a conjunction of logical conditions on the system state that must be satisfied before a certain action can be taken. For instance, it may be established to preserve system correctness, consecutive messages of a certain type, that actually correspond to actions of a specific domain, must be scheduled at a fixed time interval from one another and may only be scheduled if there are no more than a critical number of unacknowledged pending messages. The conjunction of all these conditions can form a part of a scheduling invariant which can then serve as a guard for all scheduling actions.

1.2. LITERATURE REVIEW

The challenge encountered in cyber-physical research work is integrating all the sub-systems. Issues in correctness, timing and stability in one sub-system can considerably affect the same features throughout the overall system. The prevalent practice of trying to compose cyber-physical systems based on mere functionalities of the sub-systems is not a very intelligent method of CPS design. This is because sub-systems that have been designed in isolation, may not behave as expected when they are integrated. Such unintended interactions might cause the overall system to crash. A semantically common method is required to relate all the cyber, network and physical actions. Some work towards this has been done by Acumen [3] who has tried to reduce the void between simulation codes and analytical models. Predicate transformers were used to study cyber-physical systems in dynamical systems [4] and then in [5] which describes invariant interaction and composition. The concept of non-interference of invariants for purely cyber systems has been explored in [6].

In controls literature, system stabilty is adversely affected by network congestion and studies have been done to impose bounds on system stability in terms of congestion introduced into the system [7]. This kind of stability analysis can be done by using results from switched system theory [8]. The controller is usually modeled using discrete time or continuous time state space models. With the increasing complexity of cyber-physical systems, the control becomes non trivial and it is difficult to represent the system in the same semantics as a common plant/network delay model. In this regard, hybrid automata [9] and timed I/O automata [10] exhibit an interesting mix of both continuous and discrete states. Thus, different methods used in different disciplines pose a tremendous difficulty in binding all the domains in a common semantic.

As described earlier, an invariant is a logical predicate on a system state that must remain true throughout system execution. Invariants can be used in cyber systems to check

all kinds of system correctness [11-12]. However, although they are well received in the cyber world, a lot still needs to be done to extend their usage into the physical and network domains.

In the physical domain, Lyapunov functions are well developed tools to study the dynamics of the physical system [13]. Lyapunov functions have also been used to describe complicated physical systems, such as a smart grid [14]. Lyapunov functions can be applied on a linear system (or a linearized nonlinear system) to break the continuous system response into a scalar function. While Lyapunov functions can be used to describe the stability of a certain operating mode, Lyapunov-like functions [15] can be used to address the stability problem if the system switched between these supposed "stable" operating modes.

Lyapunov functions can be used to address network stability [16-18] as well. The network congestion can be modeled as a control feedback problem, and bounds can be imposed on the number and timing of pending requests to construct Lyapunov-like functions for the network domain.

As described above, there are several tools to describe the correctness of each sub-system. What is needed now, is a way to bring together all these sub-systems in an unifying framework, ensuring that there is no interference between them.

1.3. PROPOSED APPROACH

The proposed research focuses on using Unified Invariants for an islanded electrical smart grid to show how complex interactions of advanced power electronics governed by sophisticated, distributed, cyber algorithms interconnected by adaptive network scheduling disciplines can produce a robust CPS. This dissertation primarily discusses how to develop invariants to preserve the physical system correctness. These physical system invariants can be adapted for distributed computation in a Distributed Grid Intelligence (DGI) system, to come up with fully functional non interfering cyber physical invariants to ensure correct

operation of the smart grid in its entirety. Integrating the physical system invariants with DGI would require the combined efforts of multiple disciplines which is again the crux of cyber-physical research.

1.4. CONTRIBUTION TO DATE

In paper 1, an invariant based method has been developed to monitor the voltage correctness of a smart grid type system with multiple independent entities.Voltage stability of the entire system is ensured by voltage stability at all the sub-systems. The DGI-interfaced voltage stability invariant is sufficiently equipped such that it can take necessary steps to not only predict, but also prevent a voltage collapse, at one or more sub-systems, should the need arise.

In paper 2, line flow invariants have been developed to monitor system correctness in terms of line overloading. If a transaction between two or more entities in the smart grid result in one or more lines being overloaded, system correctness is no longer maintained. The DGI-interfaced line flow invariant checks the legitimacy of every power transaction between two sub-systems, to ensure none of the lines in the system gets overloaded. Any proposed transaction that violates the invariant, is rejected, thereby preventing line overloading.

In paper 3, invariants have been developed to preserve the transient stability of a reduced order islanded microgrid type system. The transient invariant is rooted in the notion that stability of a switched system depends on sufficient relaxation time in between switching, so as to allow the system states to settle down, before they are perturbed again. Lyapunov-like functions have been used to plot the dynamics of the switched system. The transient response has been verified by performing simulations on a model of the system.

1.5. REFERENCES

[1] T. Paul, J. W. Kimball, M. Zawodniok , T. P. Roth, and B. McMillin, "Unified Invariants for Cyber-Physical Switched System Stability," *IEEE Trans. Power Syst.*, vol. 5, pp. 112–120, Jan. 2014.

[2] J. Liu, *Real-Time Systems*. Prentice Hall, 2000.

[3] Y. Zhu, E. Westbrook, J. Inoue,A. Chapoutot, C. Salama, T. Martin, W. Taha, M. O' Malley, R. Cartwright ,A. Ames, and R. Bhattacharya, "Mathematical equations as executable models of mechanical systems," in *Proc. Ist ACM/IEEE Int. Conf. Cyber-Physical Syst. (ICCPS'10)*, New York, 2010, pp. 1-11.

[4] M. Sintzoff, and F. Geurts, "Analysis of dynamical systems using prdicate transformers-attraction and composition," in *Analysis of Dynamical and Cognitive Systems Advanced Course Stockholm, Sweden, August 9-14, 1993 Proceedings*, vol. 888, Lecture Notes in Computer Science, pp. 227-260.

[5] S. Bensalem, A. Legay, T. H Nguyen, J. Sifakis, and R. Yan, "Incremental invariant generation for compositional design," in *Proc. 4th IEEE Int. Symp. Theoretical Aspects Software Eng. (TASE)*, Aug. 2010, pp. 157-167.

[6] S. Owicki, and D. Gries, "An axiomatic proof technique for parallel programs," in *Acta Informatica*, vol. 6, pp. 319-340, 1976.

[7] J. P. Hespanha, P. Naghshtabrizi, and Y. Xu, "A survey of recent results in networked control systems," in *Proc. IEEE*, vol. 95, pp. 138-162, 2007.

[8] M. C. F. Donkers, W. P. M. H. Heemels, N. V. D. Wouw, and L. Hetel, "Stability analysis of networked control systems using a switched linear systems approach," in *IEEE Trans. Autom. Control*, vol. 56, pp. 2101-2115, 2011.

[9] T. A. Henzinger, "The theory of hybrid automata," in *Proc. IEEE Symp. Logic. Comp. Sci.*, 2011, pp. 278-292.

[10] R. Alur, and D. L. Dill, "A theory of timed automata," in *Theoretical Comp. Sci.*, vol. 126, no. 2, pp. 183-235, 1994.

[11] L Zhang, and E. K. Boukas, "Stability and stabilization of Markovian jump linear systems with partly unknown transition probabilities," in *Automatica*, vol. 45, no. 2, pp. 463-468, 2009 [Online]. Available: http://www.sciencedirect.com/science/article/pii/S0005109808004512

[12] C.T. Chen, *Linear System Theory and Design*. New York: Holt, Rinehart, and Winston, 1984.

[13] M. Roozbehani, M. Dahleh andS. Mitter, "Robust and distributed decisions for future cyber-physical energy networks," in *New Res. Directions Future Cyber-Physical Energy Syst.*, June 2009 [Online]. Available: http://www.ece.cmu.edu/nsf-cps/file.php?id=87

[14] M. S. Branicky, "Multiple Lyapunov functions and other analysis tools for switched and hybrid systems," in *IEEE Trans. Autom. Control*, vol. 43, no. 4, pp. 475-482, 1998.

[15] C. A. R Hoare, "An axiomatic basis for computer programming ," *Commun. ACM*, vol. 12, no. 10, pp. 576-585, Oct. 1969.

[16] L. Massouli, "Structural properties of proportional fairness: Stability and insensitivity," *Ann. Appl. Probab.*, vol. 17, no.3, pp. 809-839, 2007.

[17] M. Zawodniok, and S. Jagannathan,"Predictive congestion control protocol for wireless sensor networks," *IEEE Trans. Wireless. Commun.*, vol. 6, no.11, pp. 3955-3963, 2007.

[18] S. Jagannathan, *Wireless Ad Hoc and Sensor networks: Protocols, Performance, and Control*, Boca Raton, FL, USA: CRC, 2007.

PAPER

I. DISTRIBUTED GRID INTELLIGENCE INTEGRATED INVARIANT BASED METHOD FOR ANALYZING VOLTAGE STABILITY IN SMART-GRIDS

Tamal Paul[1], Thomas P. Roth[2], Bruce McMillin[2], Harsha Ravindra[3], Michael Steurer[3] and Jonathan W. Kimball[1]

[1]*Department of Electrical and Computer Engineering*

Missouri University of Science & Technology, Rolla, MO, USA

[2]*Department of Computer Science*

Missouri University of Science & Technology, Rolla, MO, USA

[3]*Center for Advanced Power Systems, Florida State University, Tallahassee, FL, USA*

ABSTRACT— Voltage stability analysis is essential in any power system. This paper addresses the voltage stability in a next-generation smart grid system with multiple independent entities. A typical operation in this system involves loading excursions (changes in power, both generated and consumed) undertaken by all these independent entities. Correct behavior of all the entities (sub-systems) will ensure correct behavior of the overall system (smart grid). An invariant is a logical predicate on a system state that must remain true throughout system execution. Invariants, if forced to be true, ensure correct behavior on a subsystem level and thus preserve the overall system correctness. This paper derives an invariant that preserves voltage stability. This invariant has been adapted for distributed computation in a Distributed Grid Intelligence (DGI) system. This invariant is the next step in building a self checking, robust cyber-physical system. The DGI-interfaced invariant not only predicts the proximity of voltage collapse at one or more entities in a smart grid, but also prevents a collapse by shutting off future increases in load. The use

of the invariant in predicting voltage collapse and preventing such an occurrence has been verified with simulations performed in RTDS on a seven node smart grid system with DGI.

Index Terms— Cyber-Physical System, distributed-grid intelligence, invariants, smart grid, stability, voltage

1.1. INTRODUCTION

Voltage stability is of utmost importance to power system operation. Drop in voltage levels poses serious concerns in electric utilities and appliances. According to ANSI standards, system voltages should not drop below 5% their nominal value for a satisfactory operation of the power system [1, 2, 3]. Any study on voltage stability of a power system should investigate how close the system voltage is to collapsing, at what precise moment does the collapse occur, what are the vulnerable areas in the system and what are the factors contributing to this collapse. Analysis and operation are more complex when control of system elements is distributed, rather than centralized.

The problem of voltage stability can be attributed to the inability of the system to cater to the reactive power needs of its elements [4]. Studies undertaken to analyze voltage stability require careful investigation of a large number of system states and contingency situations. This makes a steady state approach seem more feasible. Literature studies reveal special algorithms that target the voltage stability problem using static methods [5]. However, such studies are labor intensive and fail to provide sensitivity information. Certain operators make use of the Q-V curve at some of the independent entities to determine the proximity of voltage instability [6]. The major drawback of such an approach is that the excessive focus on a small number of local components fails to provide information about the overall system-level voltage stability. Voltage instability leads to a progressive (or periodic) fall (or rise) in voltage of the system. As mentioned earlier, this loss of voltage

stability stems from the inability of the system to supply the reactive power needed by one or more independent entities. A voltage decay/fall in the system is usually caused by an increase in loading or change in system conditions at one or more entities thereby causing an excessive increase in reactive power demand which the system is unable to meet. Thus the loading pattern of the individual components affects the system-level voltage stability. This emphasizes the importance of enforcing voltage stability constraints at the subsystem level in order to ensure proper functioning of the overall system and eliminate the possibility of voltage collapse in the system.

One vision of the future of the electric smart grid is an environment where an energy internet manages energy assets on a peer-to-peer basis, allowing for local and mobile use of renewables. The technology to support this vision is being pursued both in academic research [7] and in industry [8, 9, 10]. Rather than being generated and managed centrally, power will be generated, consumed, and its energy stored locally. Current power generation, management, and consumption are well understood and supported by a hundred years of analysis, experience, and practice. Power generation is carefully managed so that the voltage and frequency of the electric power system remain within strict limits. The current smart grid is an incremental effort, initially involving remote meter reading and remote management of home appliances. The next generation smart-grid in this paper, as illustrated in Fig. 1.1 [7], is not a closed system, but instead allows for electric power generation from a multitude of largely unregulated sources. The potential for system instability is staggering: uncoordinated power generation from intermittent sources such as wind and solar can cause the power grid to collapse, resulting in extended blackouts and potential equipment damage with significant impact on society.

A microgrid is a particular category under the smart grid umbrella, in which interconnected loads and distributed energy resources can operate with or without connection to the main power transmission system. A smart-grid forms a microgrid of distributed energy storage devices (DESDs) distributed renewable energy resources (DRERs), and LOADs
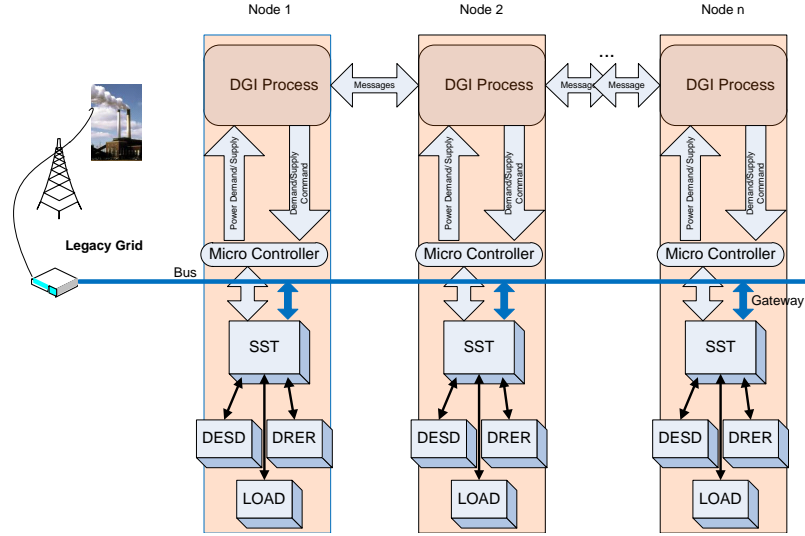
Figure 1.1. Power Management Archictecture [7].

(programmable and non-programmable loads) to share power for the good of the entire system. Intelligent flow controllers (Nodes) contain physical actuators such as solid state transformers (SSTs) that control power flow to and from a shared electrical bus, under direction of cooperating Distributed Grid Intelligence (DGI) Processes. This paper begins with the derivation of an invariant that may be used to monitor and enforce voltage stability. As used in the present work, an invariant is a logical statement whose truth value indicates the correctness of a system [1]. The concept is well-established in computational system analysis, and the present work further extends the concept in a cyber-physical system. The National Institute for Standards and Technology defines cyber-physical systems as "co-engineered interacting networks of physical and computational components" [12]. After deriving an invariant that indicates voltage stability, a method for integrating it with a cyber controller is derived. The invariant is used as a guard, that is, actions that would invalidate the invariant are prevented. Simulations, including hardware-in-the-loop (HIL) simulations with actual distributed cyber controllers, validate the approach.

1.2. INVARIANT TO MONITOR VOLTAGE COLLAPSE

One of the key indicators of a healthy power distribution system is steady voltage levels at all of its buses. The system is planned to operate in such a way that whenever there is an increased demand in load at one or more entities, the generators in the system cater to that increased load by regulating the reactive resources in the system. This remedial control action that restores system voltage levels in the event of change in loading conditions may include automatic response of the generator excitation systems, automatic or manual excitation of transformer taps and the switching of STATCOMs in the circuit.

However, under extreme conditions of loading, the remedial action which earlier restored the voltage stability might now very well reduce an already low voltage to abnormally low levels, or may be too slow. Such low voltage levels are not acceptable and might interrupt the continuity of electricity supply. This chain of events leading to a voltage collapse takes place in a matter of seconds and causes the entire system to shut down. This poses a serious threat to power systems and poses a challenge to power system engineers to identify conditions or vulnerable areas in the system that might lead to a voltage collapse at one or more entities and thus shut the entire system down.

Voltage collapse is caused by insufficient reactive power, either a lack of enough reactive power in the system to deliver the active power or too much consumption of reactive power within the system itself. This happens in stressed power systems. A system may enter the state of voltage collapse when an increase in load demand at one or more buses or change in system conditions causes an unrecoverable decrease in one or both bus voltages. Once the voltage at one or more entities (buses) starts to fall, recovery to normal operation is difficult. Various system elements will begin to respond to the low voltage, either accelerating the collapse, tripping individual loads, or creating local blackouts. Thus, identifying the proximity of the system to the voltage collapse point is of crucial importance. The voltage collapse proximity indicator L [6] is a quantitative measure to predict

how far the current state of the system is from the voltage collapse point. The value of L ranges between 0 (no load) and 1 (voltage collapse). This means as L approaches 1, the system approaches the brink of voltage collapse. The voltage collapse proximity indicator (L_j) for any bus is mainly influenced by the load at that bus itself, with additional influence from other system entities. For any load bus j, L_j can be given as [14] the set of equations described in (1.1) and (1.2) where N is the total number of load buses, S_j and S_i are the complex power consumption at buses j and i, V_j and V_i are the voltages at buses j and i, Y_{jj} is the jj^{th} element of the bus admittance matrix and Z_{jj}^* and Z_{ji}^* are the conjugate of the jj^{th} and ji^{th} elements of the bus impedance matrix of the system.

$$L_j = \frac{S_j'}{V_j^2 Y_{jj}} \tag{1.1}$$

$$S_j' = S_j + \Sigma_{i=1, i\neq j}^{N} \frac{Z_{ji}^* S_i}{Z_{jj}^* V_i} V_j \tag{1.2}$$

The maximum value of the indicator for all the independent entities is called the "System Indicator" as denoted in equation (1.3). The System Indicator indicates the overall health of the system.

$$L_{System} = Max_{i\in\{1\cdots N\}} L_j \tag{1.3}$$

The indicator for voltage collapse proximity at a load bus is mainly influenced by the load at bus j itself and partially influenced by loads at other buses. The value of L_{System} indicates the proximity to voltage collapse of the entire system.

When the load is increased by a certain entity, the indicator at the corresponding bus and at other buses starts to increase. To avoid voltage collapse, the per-unit voltage at any bus should always be greater than the indicator for any bus. There comes a point where the indicator for one bus intersects the per-unit voltage of a certain bus, either its own or

another bus in the system. This point is called the "online monitored voltage collapse indication point" where L_{System} approaches unity thereby indicating that the voltage collapse is imminent. Ideally, the "online monitored voltage collapse indication point" should precede the voltage collapse point, or even the point where the voltage at one or more buses drops below 5% of the nominal level as per ANSI standards [1]. Thus the invariant to preserve system level voltage stability can be formulated in words as: The maximum indicator for all the independent entities must be always less than the minimum per-unit voltage for all the independent entities in the smart grid. Or mathematically

$$\{I_V : L_{System} < V_i \ \forall \ i\} \tag{1.4}$$

The physical system invariant described (1.4) above can be adapted for distributed computation in the DGI system using the distributed energy management algorithm outlined in [13]. Thus it is possible to perform an online check as long as the system is running to monitor the system health in terms of voltage stability and be forewarned should the invariant indicate an impending voltage collapse. This DGI integrated invariant based method not only predicts an imminent voltage collapse but can also prevent such an event by regulating the smart grid accordingly.

1.3. VALIDATION OF THE PHYSICAL INVARIANT

Before integrating the invariant into the cyber controller, simulations were performed to validate its accuracy and suitability. A preliminary version of these results was presented in [16]. The model was simulated using RTDS[®][1] as shown in Fig. 1.2. The feeder has seven lumped loads connected through seven average value model based load SSTs. The feeder is rated at 12.47 kV and is an islanded, looped system. The loads are served primarily by two diesel generators.

---

[1]RTDS[®] is a registered trademark of RTDS Technologies
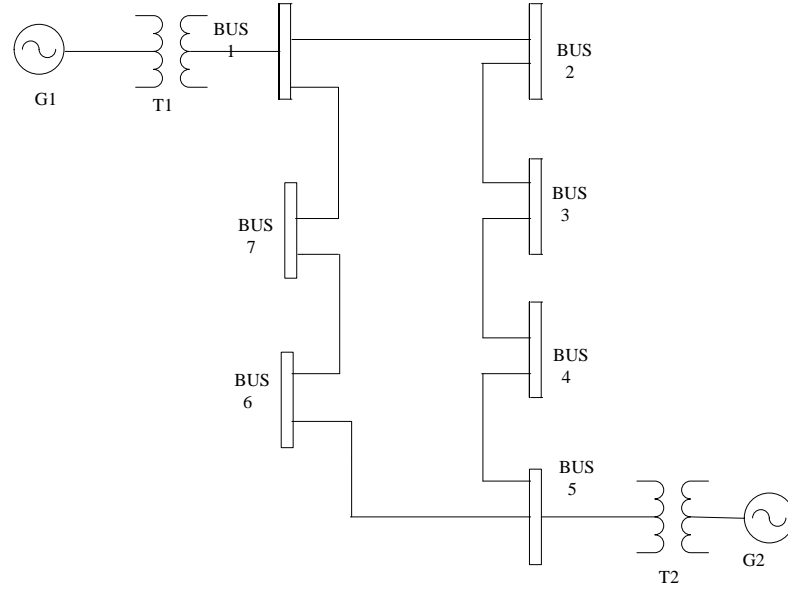
Figure 1.2. Single line diagram of the 7 bus system.

Although the feeder is looped, it could be operated in radial mode. The two diesel generators are rated at 1.4 MVA each. One of them operates in droop mode (G2) while the other operates in isochronous mode (G1). The feeder primary is made up of seven line sections. The impedance of each line section is identical. Each load SST is rated at 285 kVA. On the secondary of each load SST, there is a lumped load, lumped distributed generation (DG) and storage connected. The generators are rated at 1.4 MVA, $380V_{L-N}$. The transformers are rated at 1.5 MVA, 0.38 kV: 12.47 kV. The transmission lines have a positive sequence resistance of 0.77 Ω, positive sequence inductance of 1.967 mH, zero sequence resistance of 2.31 Ω and a zero sequence inductance of 5.9 mH. The droop generator is set to run at 400 kW at 5% droop. The voltage stability of the system can be analyzed by monitoring the online voltage collapse proximity indicator, L_{System}. The initial loading at all the buses is maintained at 205 kW. The loading at bus 1 is increased in steps as the simulation progresses while all the other busess are maintained at their initial loading level.

The solid blue line indicates bus 4 per-unit voltage and solid red line is the indicator for bus 4 (L_4) in Fig. 1.3. The solid blue line indicates per unit voltage of bus 4 and the solid green line is the indicator for bus 1 (L_1) in Fig. 1.4.
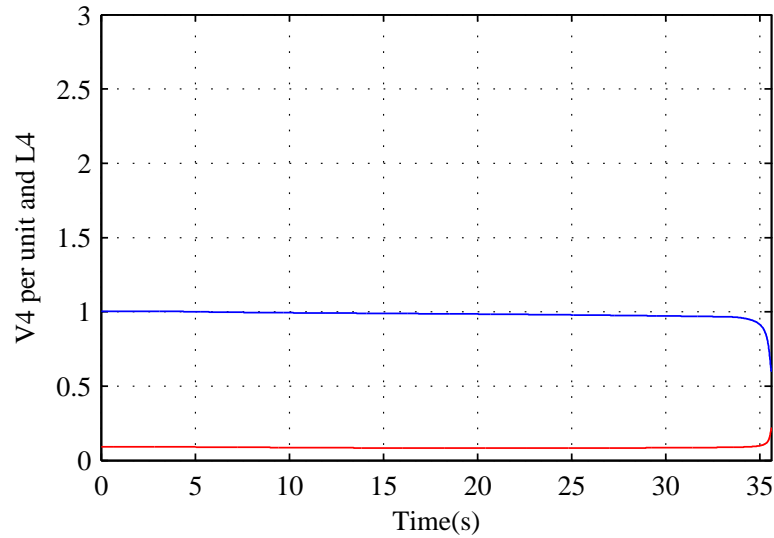
Figure 1.3. Change in V_4 and L_4 as loading at bus 1 increases.
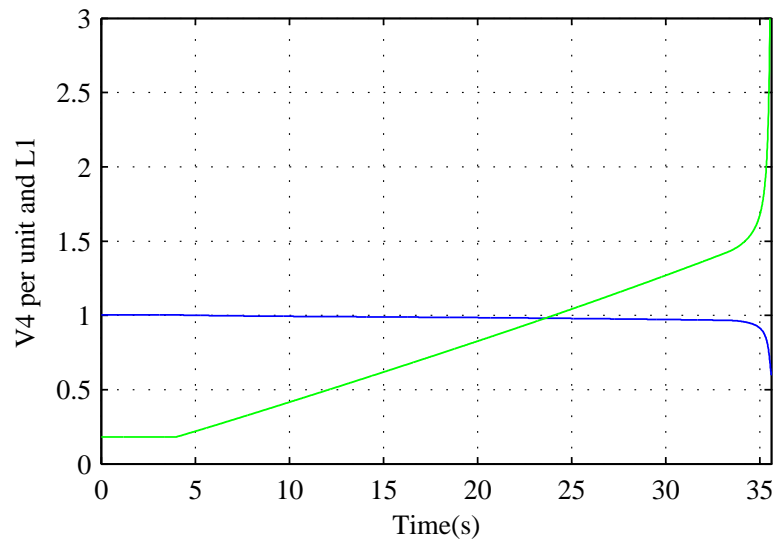
Figure 1.4. Change in V_4 and L_1 as loading at bus 1 increases.

It is seen that bus 4 collapses at 34.67 seconds when the system loading is 2.698 MW. L4 never intersects the per-unit voltage curve; L_1 however intersects the per unit

voltage at around 24 s when the system loading is 2.235 MW. This is the "online monitored voltage collapse indication point" where the invariant is violated. If loading is continued beyond this point, the voltage collapses shortly and eventually the system totally crashes as depicted in Fig. 1.4. Although the indicator for bus 4 does not indicate voltage collapse when approaching the voltage collapse point, the other indicator (L_1) indicates an invariant violation. This indicates the importance of using L_{System}, that is, choosing the maximum value of all indicators to determine the voltage collapse point of the overall system.

In the absence of the droop, the system collapses for a much lower load as demonstrated in Fig. 1.5. In this case, the loading at bus 1 is increased from 205 kW but loads at all other buses are maintained at 0. The droop generator is removed from the system. This voltage collapse is because the second generator no longer supplies the deficit in reactive power for the system. The only generator in the model supplying reactive power quickly reaches its limit, causing a voltage collapse as shown in Fig. 1.6. The indicator for bus 1 intersects the voltage curve and indicates imminent collapse. The voltage collapses because of a deficit of reactive power because the reactive power needed to maintain the bus voltages within acceptable levels increases with increased loading.

1.4. PHYSICAL INVARIANT INTEGRATION WITH DGI

The DGI system can compute the values of the physical invariant when the system is operating. Seven DGI processes, one for each SST in the system, were run across five Linux machines and made to communicate over UDP/IP sockets. Each process reads its associated bus's voltage and complex power from the simulation every 50 milliseconds. Prior to that, all processes were initialized with knowledge of the physical system topology that included the bus admittance and impedance matrices required to calculate the invariant. Due to the distributed nature of the system, each process communicated with its peers over TCP/IP to learn the current values of complex power and voltage at the other buses.
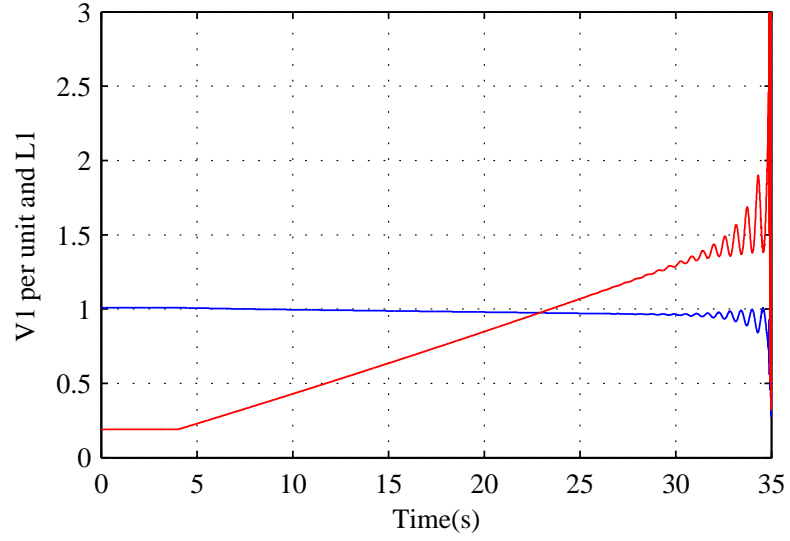
Figure 1.5. Plot of V_1 and L_1 against time with increased loading at bus 1 for the system with no droop generator.
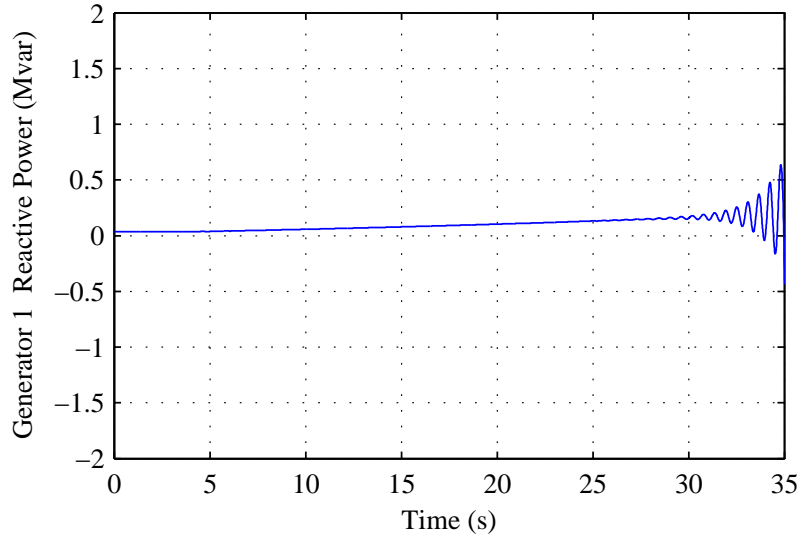
Figure 1.6. Plot of generator 1 reactive power against time with increased loading at bus 1.

With this set-up, each process can calculate the current value of the invariant during the simulation. It is thus possible to have an online invariant based monitoring method to analyze the voltage stability in the smart grid. In the HIL simulation, the RTDS simulation is coupled with a DGI energy management algorithm [13] that attempts to co-ordinate

increases in generation and load at two buses in the system. For the experiments conducted in this study, the initial loadings at all the buses are maintained at 205 kW (through SSTs). The loading at bus 1 is increased in steps by the corresponding SST as the simulation progresses while all the other SSTs are maintained at their initial loading level. The total system loading is the summation of the loading at each bus.

The loading conditions as described in the previous paragraph were established in conjunction with DGI. For that, the process that corresponds to SST 1 was set to increase its load during the course of the simulation. If the processes followed the energy management algorithm in [13], then a second SST would have had to make corresponding increases to generation and the isochronous generator would maintain a constant amount of generation. To prevent this, the other six processes were modified to run a malicious version of the energy management algorithm where the bus generation is never increased. This keeps the generation and load at buses 2 through 7 constant, while loading at bus 1 increases over time.

Since each process has enough information to calculate the invariant, the invariant calculation integrates into the distributed energy algorithm. Each process calculates locally the exact equation described in (1.1) and (1.2) using a combination of local values, the system topology values for the bus matrices it was initialized with and the voltages and complex powers it receives from TCP/IP communication with its peers. The load side of the energy management algorithm resembles the simplified flowchart in Fig.1.7. The virtual load corresponds to the script that controls the state of the energy resources at a bus over time. For instance, the SST at bus 1 is configured to have increasing load over time. So the process associated with SST 1 sees an increase in virtual load that it would then enact in RTDS. The actual energy management algorithm is much more complicated than this flowchart which only provides a skeleton of the code [13].

With the malicious DGI at the other nodes, the SST at bus 1 increases its load while the other SSTs maintain constant load and generation. This imbalance leads to an increase
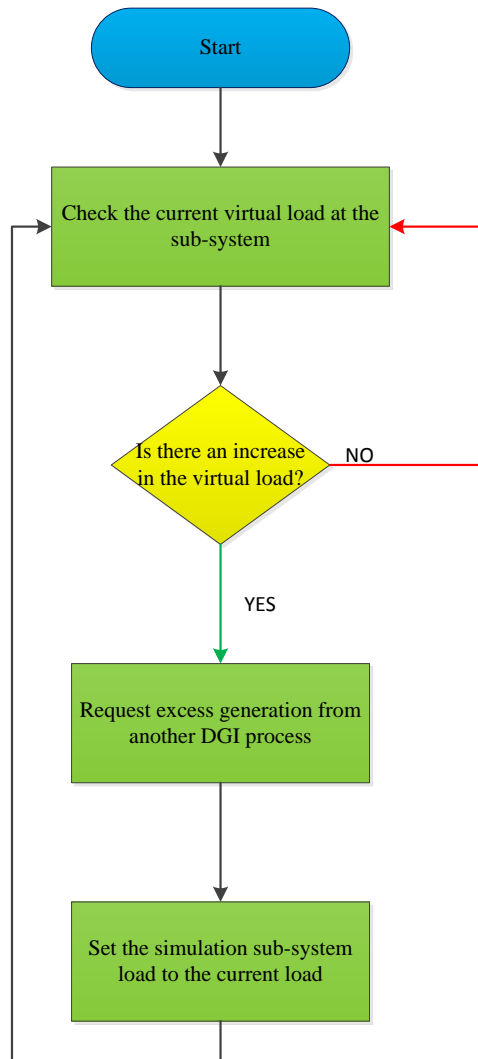
Figure 1.7. Flowchart for energy management algorithm without the invariant guard.

in total system load over time. The increase is large enough to lead to an invariant violation which will eventually drive the system to voltage collapse. Results are indicated in Fig. 1.8. The first plot shows the impact of the energy management algorithm on the overall system loading without the invariant guard, as described by the flowchart in Fig. 1.7.

During the earlier part of the simulation, the invariant is satisfied, as shown in the third plot in Fig. 1.8. A truth value of 1 indicates that the invariant has been satisfied

while a value of 0 indicates invariant has been violated. As the system loading continues

to increase, the invariant gets violated at a certain point in the simulation. This happens

around 48*s* when the system loading is around 2.24 MW. An invariant violation does not
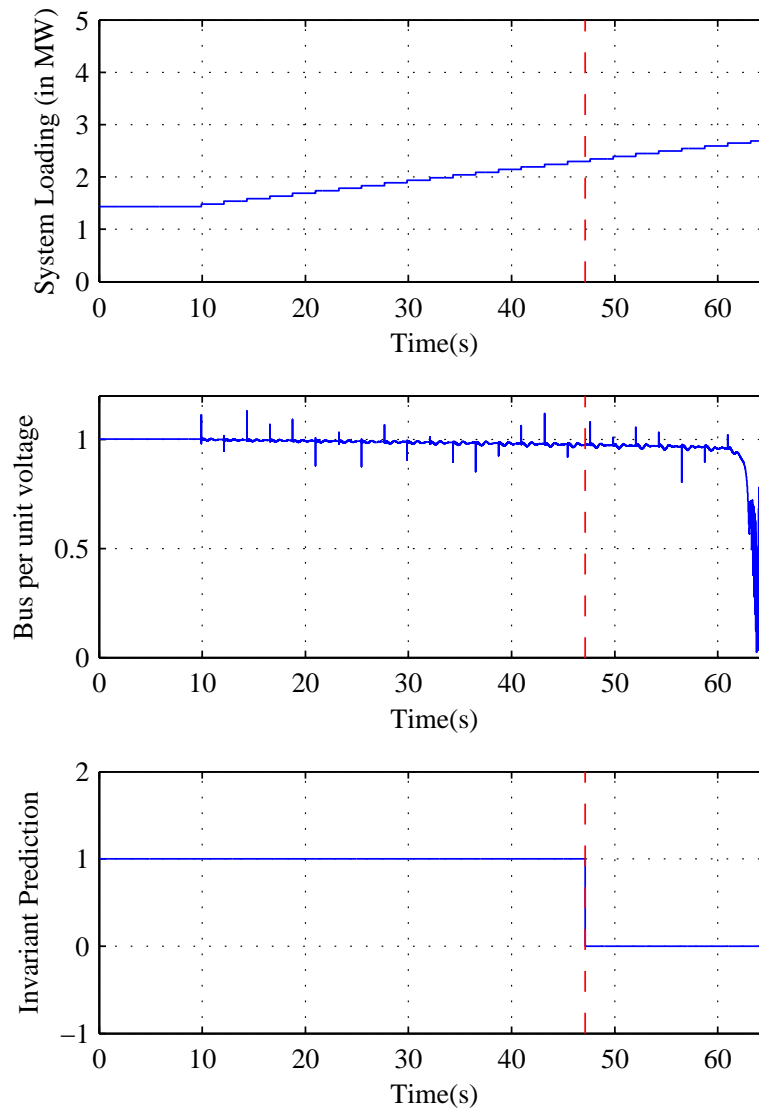
Figure 1.8. Simulated microgrid performance in response to energy management algorithm
without invariant guard, indicating voltage instability due to excessive power migration, as
predicted by the invariant ahead of time.

correspond to an immediate voltage collapse, but instead indicates an impending collapse. If the system loading continues to increase, the system voltage does go on to collapse as shown in the second plot in Fig. 1.8.

The energy management algorithm described in Fig. 1.7 does not use the invariant calculation. As a result, the process corresponding to SST 1 continues to increase its load throughout the entire simulation runtime despite the invariant violation. If the process had reacted to the invariant violation, it might have been possible to avert an impending voltage collapse. This corrective action has been implemented in the next section.

1.4.1. Invariant guard against offending migrations. The result of the invariant calculation can be added as an extra condition in the energy management algorithm as shown in Fig. 1.9. Fig. 1.10 shows the result of this change on the RTDS simulation.

This change prevents the process from changing the value of an SST's commanded power when the invariant has been violated. So even though SST 1 is configured to have an increasing load over time, its associated DGI process will cease to increase the load in RTDS if the invariant is false. In an actual power system, this would be similar to an act of load shedding, in that a bus disconnects some of its load to prevent an increase that would compromise voltage stability. It is therefore possible to use the results of the invariant calculation to stop a power migration that has the potential to drive the system to voltage instability.

At 48s when the invariant has been violated, the system loading stops increasing as shown in the first plot in Fig. 1.10. This is because the process associated with SST 1, in response to an invariant violation, stops sending increased load commands to the simulation. Unlike in Fig. 1.8, the second plot in Fig. 1.10. shows that there is no voltage collapse when the energy management algorithm is extended to use the invariant result to stop an offending migration.

In the event that the invariant has been violated, a DGI-interfaced invariant based method is able to exert corrective action so as to suspend all future power transactions

and prevent the system voltage from collapsing. The invariant not only signals when the system is on the brink of a voltage collapse but also acts as a guard to prevent the system into entering such an undesirable state. Thus in a transaction based [17] power system, each and every customer's obligation can be determined using the DGI interfaced invariant.
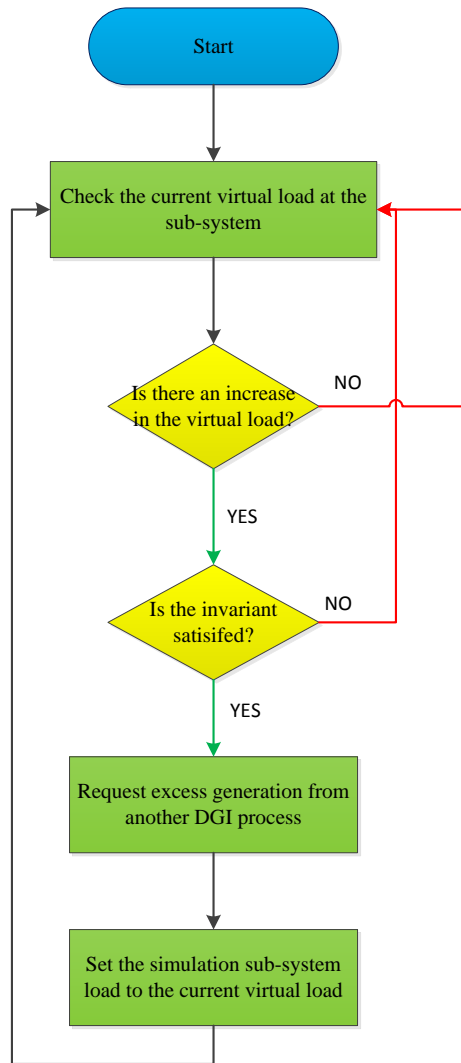
Figure 1.9. Flowchart for energy management algorithm with the invariant guard.
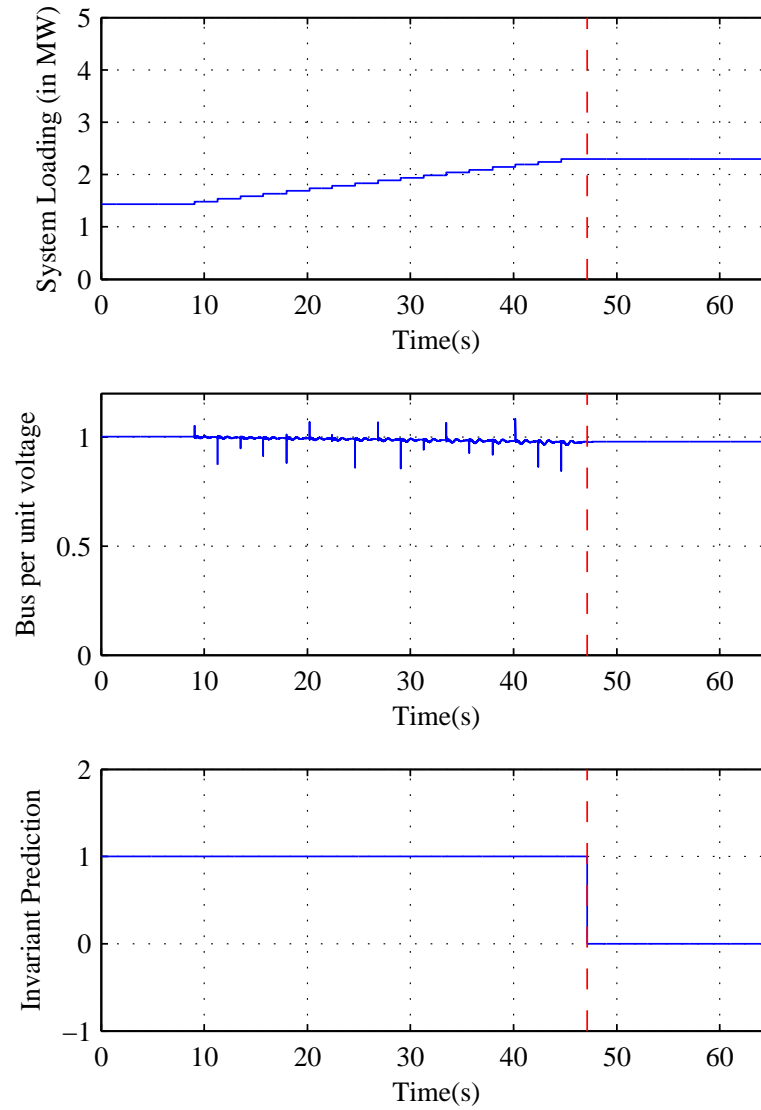
Figure 1.10. Simulated microgrid performance in response to energy management algorithm where the invariant guards the migration, preventing voltage instability.

1.5. CONCLUSION AND FUTURE WORK

An invariant which predicts the proximity of voltage collapse in a smart grid type setting has been presented. This invariant is based on a real time online monitoring of

system parameters. The invariant has been integrated with distributed grid intelligence to check the status of the system in terms of voltage stability. The invariant can be suitably modified to provide insight about the system voltage stability in the absence of current/live system values. The efficacy of the invariant in predicting voltage collapse has been verified with experimental simulations. Should loading be continued any further, the system does go on to collapse. The invariant thus is useful in locating the vulnerable locations in the system. The integration of the invariant with DGI not only helps to identify the proximity of voltage collapse in the smart grid, but also takes affirmative actions to mitigate such a collapse.

This method is the next step towards building a robust, self- checking, distributed cyber-physical system. Integrating invariants into control algorithms will ensure that the system is operating correctly, even in the presence of intruders, corrupted data, software coding errors, etc.

1.6. REFERENCES

[1] "American National Standards for Electric Power Systems and Equipment-Voltage Ratings (60 Hertz)", National Electrical Manufacturers Association ANSI C84.1-2011.

[2] A. Kusko, and M. Thompson, *Power Quality in Electrical Systems*. New York: Mcgraw-Hill, 2007.

[3] Pacific Gas and Electric Company, "Voltage Tolerance Boundary," accessed on April 22, 2015.

[4] J. A. Diaz de Leon II, and C. W. Taylor, "Undertsanding and solving short term voltage stability problems," *Power Engineering Society Summer Meeting, 2002. IEEE*, pp. 745–752, 2002.

[5] C. A. Aumuller, and T. K. Saha, "Investigating the impact of Powerformer on voltage stability by dynamic simulation," *IEEE Trans. Power Syst.*, vol. 18, no. 2, pp. 1142–1148, Aug. 2003.

[6] G. M. Huang, and K. Men, "Contribution allocation for voltage stability in deregulated power systems," *Power Engineering Society Summer Meeting, 2002. IEEE*,vol. 3, pp.1290–1295, 2002.

[7] A. Q. Huang, M. L. Crow, G. T. Heydt , J. P. Zheng, and S. J. Dale, 'The future renewable electric energy delivery and management (FREEDM) system: The energy internet," *Proc. IEEE*, vol. 99, pp. 133–148, Jan. 2011.

[8] SGIP, "Smart Grid Interoperability Panel (SGIP) Announces the Open Field Message Bus (OpenFMB) Project," accessed on April 22, 2015, http://www.sgip.org/022015-Release-OpenFMB.

[9] S. Laval and B. Godwin, "Distributed Intelligence Platform (DIP) Reference Architecture Volume 1: Vision Overview," Duke Energy, Jan. 5, 2015.

[10] Burns and McDonnell, "SPIDERS: Smart Power Infrastructure Demonstration for Energy Reliability and Security," accessed on April 22, 2015, http://www.burnsmcd.com/Resources/Article/SPIDERS-Smart-Power-Infrastructure-Demonstration-for-Energy-Reliability-and-Security.

[11] T. Paul, J. W. Kimball, M. Zawodniok , T. P. Roth, and B. McMillin, "Unified Invariants for Cyber-Physical Switched System Stability," *IEEE Trans. Power Syst.*, vol. 5, pp. 112–120, Jan. 2014.

[12] National Institute of Standards and Technology, "Cyber-Physical Systems," accessed on April 22, 2015, http://www.nist.gov/cps/.

[13] A. J. Wood, and B. F. Thompson, *Power Generation, Operation and Control*. New York: Wiley, 1996.

[14] I. Kumaraswamy, W. V. Jahnavi, T. Devaraju, and P. Ramesh, "An Optimal Power Flow (OPF) Method with Improved Voltage Stability Analysis," in *Proc. World Congress on Engineering*, 2012, vol. II, pp. 1028–1035.

[15] R. Akella, F. Meng, D. Ditch , B. McMillin, and M. L. Crow, "Distributed Power Balancing for the (FREEDM) System," *First IEEE International Conference on Smart Grid Communications (SmartGridComm),* , 2010, pp. 7-12.

[16] T. Paul, H. Ravindra, M. Steurer, and J. W. Kimball, "Voltage stability preserving invariants for smart grids," *Power and Energy Conference at Illinois* , 2015, pp. 1-6.

[17] H. Kazari, A. Abbaspour-Tehrani Fard,A. S. Dobakhshari, and A. M. Ranjbar, "Voltage stability improvement through centralized reactive power management on the Smart Grid," *IEEE PES Innovative Smart Grid Technologies* , 2012, pp. 1-7.

II. DISTRIBUTED GRID INTELLIGENCE ENABLED LINE FLOW INVARIANTS FOR TRANSACTION BASED SMART-GRIDS

Tamal Paul[1], Thomas P. Roth[2], Bruce McMillin[2], Harsha Ravindra[3], Michael Steurer[3] and Jonathan W. Kimball[1]

[1]*Department of Electrical and Computer Engineering*

Missouri University of Science & Technology, Rolla, MO, USA

[2]*Department of Computer Science*

Missouri University of Science & Technology, Rolla, MO, USA

[3]*Center for Advanced Power Systems, Florida State University, Tallahassee, FL, USA*

ABSTRACT— With the ever increasing size and complexities of smart grids, system operations are moving towards a decentralized structure. In a decentralized smart grid, there are multiple independent entities (buyers and sellers) involved in bilateral or multilateral power transactions over the smart grid transmission network. During such power transactions, it is important that no line in the transmission line network becomes overloaded. Among other restrictions, system correctness requires that no lines be overloaded. Line overloading is an undesirable phenomenon, as it might cause one/more lines to go out of service, thereby interrupting the continuity of power supply. Invariants can be used as a guard to prevent transactions that would overload a line. An invariant is a logical predicate that must remain true throughout system execution [1]. This paper investigates the use of line flow invariant to find the maximum allowable power transaction between two or more transacting entities without overloading any line in the system. The invariant has been adapted for distributed computation in a Distributed Grid Intelligence (DGI) system. The DGI-enabled invariant not only checks the legitimacy of a power transaction between two sub-systems, but also prevents lines in the system from being overloaded. The suitability of the invariant has been tested on a seven node system with simulations performed in RTDS.

Index Terms— Available transfer capability, invariants, power transfer distribution factor, smart grid, transaction.

2.1. INTRODUCTION

With the deregulation of the power markets, there has been an increase in opportunities for decentralized control of power flow [2]. Whereas a central controller can enforce line limits directly, a decentralized control architecture needs extra information to ensure that power transactions are appropriate [3]. The concept of Available Transfer Capability (ATC) has been used in the past in this regard [4]. ATC calculations give an effective estimation of the capability of the interconnected system to stay in service while being subjected to bilateral or multilateral power transactions between several generation and load entities as has been highlighted in [5]. This property of the ATC can be exploited to determine if inter area power exchanges between potential transacting entities compromise the system security. In a transaction based system, any two subsystems are involved in power transactions. These transactions cause a change in power flow in the lines in the system. The concept of ATC can be used to develop line flow invariants which will prevent a transaction that can overload transmission lines in the system.

An invariant, as the term is used in the present work and in [1], is a logical predicate that must remain true throughout system execution. This use of the term derives from computer science concepts and allows for automatic verification that the system is operating correctly. The present goal, as in [1], is to derive an invariant that could be used by a cyber controller in the smart grid to ensure that a certain transaction does not cause any of the lines in the network to go out of service due to overloading.

The first step in developing such invariants is to exploit the relationship between a certain transaction and the consequent change in line flow. This is accomplished by employing the concept of Power Transfer Distribution Factors (PTDFs) [6]. The capacity to

apportion power flows on transmission lines in a power system is the basis of North American Electric Reliability Corporation's (NERC) "flow based" transmission allocation system [7]. In such a system, the power flows allotted to each transmission line in the network are a certain fraction of the actual power transaction between any transacting entities. The linear DC Power Transfer Distribution Factors (DCPTDFs), based on the assumption of a dc power flow method [8], are used to allocate power flows on the transmission lines for a certain transaction in the system. DCPTDFs are used to compute ATC, which is used to formulate the line flow invariants.

The future of the electrical smart grid is an environment where the energy internet manages an advanced smart grid on a peer-to-peer basis, allowing for local or mobile use of renewables [3]. Instead of having central generation or management, the smart grid now has local generation and consumption of power and local energy storage. The current power generation, management and consumption are well understood and supported by a hundred years of analysis, practice and experience. Adequate care is taken to manage the power so that the voltage, line flows and frequency of the electrical power system stay within prescribed limits. The current smart grid is an incremental effort that initially depended on remote meter reading and remote management of home appliances. There are ways to make the grid "smarter". As has been elaborated in [3], an energy internet which is not a closed system will allow electric power generation from a multitude of largely unregulated sources. However there is a grim possibility of system instability: uncoordinated power generation from the intermittent sources such as wind or solar can cause the smart grid to collapse. This will have catastrophic effects such as prolonged blackouts and potential damage to equipments which in turn has a tremendous adverse social impact.

Consider the architecture of a future generation smart grid system shown in Fig. 2.1 [3]. A smart grid forms a microgrid of distributed energy storage devices (DESD) distributed renewable energy resources (DRER), and LOADs (programmable and non-programmable loads) to share power for the good of the entire system. Intelligent flow

controllers (Nodes) contain physical actuators such as solid state transformers (SSTs) that control power flow to and from a shared electrical bus, under direction of cooperating Distributed Grid Intelligence Processes (DGI).
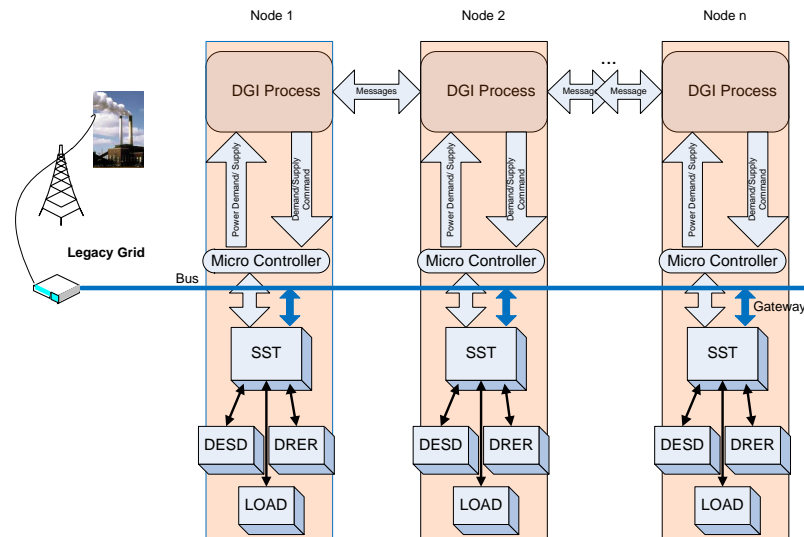
Figure 2.1. Power Management Archictecture [3].

2.2. PTDF ESTIMATION IN A TRANSACTION BASED SYSTEM

In a smart grid with several independent sub systems, a transaction can be defined as injection of a certain amount of power at one bus by a generator and its absorption at another bus by a load. The Power Transfer Distribution Factor (PTDF) can be described as incremental distribution factors associated with power transaction between any two entities. These values provide a linearized approximation of how the flow on the transmission lines changes in response to a transaction between a buyer and a seller. PTDFs can also be called sensitivity factors as they represent the relationship between one kind of change (change in transaction quantity between two entities) to another kind of change (change in power flow in any line connecting any two entities in the system). PTDFs are defined as the fraction of the amount of power transaction between transacting entities m and n that flows in the

transmission lines connecting entities i and j. The relation between change in line flow (ΔP_{ij}^{New}) due to a power transaction (ΔP_{mn}^{New}) between entities m and n is given by (2.1).

$$PTDF_{ij,mn} = \frac{\Delta P_{ij}^{New}}{\Delta P_{mn}^{New}} \qquad (2.1)$$

In this work, DC load flow model is used to estimate PTDFs. The DC load flow model [10] is a reasonable first approximation for a realistic power system model. A DC load flow model is fast and computationally less intensive to work with. The DCPTDF's are calculated using direct current power flow equations [11]. These distribution factors represent a change in line flow connecting entities i and j due to a change in transaction between components m and n. The PTDFs are be used to compute the change in line flow connecting entities i and j due to a change in transaction between components m and n. The theory behind calculating PTDFs is to compute the reactance matrix, based on DC power flow. One node of the impedance matrix is considered to be the reference node (usually the slack bus node) by making its angle zero and deleting the corresponding row and column [12]. The inverse of this matrix now gives the reactance matrix. If there is a power transaction between sub-systems m and n, then the relative change in line flow connecting buses i and j is denoted as $PTDF_{ij,mn}$. It can be mathematically represented as (2.2) where $X_{im}=(i,m)^{th}$ element, $X_{jm}=(j,m)^{th}$ element, $X_{in}=(i,n)^{th}$ element, $X_{jn}=(j,n)^{th}$ element and x_{ij} is the reactance of the transmission lines connecting i and j [12].

$$PTDF_{ij,mn} = \frac{X_{im} - X_{jm} - X_{in} - X_{jn}}{x_{ij}} \qquad (2.2)$$

2.3. ATC BASED LINE INVARIANTS

The Available Transfer Capability (ATC) is evaluated by realizing the new flow on the line connecting entities i and j due to a transaction between buses m and n. The new

flow on the line connecting entities i and j is the sum of the original base flow of the line and the change due to the new transaction between entities m and n. This can be written as:

$$P_{ij}^{New} = P_{ij}^0 + \Delta P_{ij}^{New} \tag{2.3}$$

Substituing (2.1) in (2.3), (2.3) can be rewritten as:

$$P_{ij}^{New} = P_{ij}^0 + PTDF_{ij,mn} P_{mn}^{New} \tag{2.4}$$

The maximum power that can be transferred between any two transacting entities (P_{mn}^{New}) without overloading a certain transmission line ij can be found by rewriting (2.4) as:

$$P_{mn}^{New} = P_{ij,mn}^{Max} = \frac{P_{ij}^{Max} - P_{ij}^0}{PTDF_{ij,mn}}; PTDF_{ij,mn} > 0 \tag{2.5}$$

$$P_{mn}^{New} = \infty; PTDF_{ij,mn} = 0 \tag{2.6}$$

$$P_{mn}^{New} = P_{ij,mn}^{Max} = \frac{-P_{ij}^{Max} - P_{ij}^0}{PTDF_{ij,mn}}; PTDF_{ij,mn} < 0 \tag{2.7}$$

Thus, the maximum power that can be transferred between any two transacting entities m and n for any combination of ij in the system can be evaluated. The minimum of these values gives the maximum allowable transaction between any two sub-systems without overloading a line. This can be mathematically represented as:

$$\{ATC_{mn} = Min(P_{ij,mn}^{Max}) \ \forall \ i\} \tag{2.8}$$

The ATC evaluated in (2.8) is valid only when there is one pair of transacting entities. When more than two parties are in transaction mode simultaneously, the base line

flows change. If there are l transactions between entities $m1$ and $n1$; $m2$ and $n2$; $\ldots$, ml and nl of magnitudes $x1, x2 \ldots xl$, then the base line flows on all lines can be expressed as in (2.9). P_{ij}^0 is a single column matrix that denotes the base line flow of all lines in the system where each row represents a transmission line. Thus the number of rows in this matrix is equal to the number of lines in the system. $PTDF_{ij,mn}$ is also a single column matrix. Each row entry in this matrix is the relative change in line flow connecting buses i and j when there is a transaction between sub-systems $m1$ and $n1$. Thus the number of rows of this matrix is also determined by the number of lines in the system. The same explanation can be extended for the other entries in the first matrix on the right of (2.9).

$$[P_{ij}^0] = [PTDF_{ij,m1n1}, PTDF_{ij,m2n2} \cdots, PTDF_{ij,m2n2}][x_1, x_2 \cdots, x_l]' \qquad (2.9)$$

The ATC for all the transacting entities can now be evaluated. The ATCs can act as line flow invariants to monitor the system correctness. Among other restrictions, system correctness requires that no lines be overloaded. If none of the transmission lines in the system are overloaded, system correctness is preserved. If a transaction between two or more entities result in one or more lines being overloaded, system correctness is no longer maintained. This invariant can be used to check if any proposed transaction between any two independent entities in the system maintains system correctness. The invariant can be formulated as: *The proposed transaction is less than the ATC for the two transacting parties.* The ATC for every pair of entities can be computed ahead of time, and then used real time as guard against transactions.

The physical invariant described in (2.8) can be adapted for distributed computation in the DGI system using the distributed energy management algorithm described in [13]. When two sub-systems are transacting, the DGI enabled invariant based method not only checks for a good or bad transaction, but can also stop a bad transaction, thereby preventing line overloading.

2.4. VALIDATION OF THE LINE INVARIANT

The model was simulated using RTDS® as shown in Fig. 2.2. The feeder has seven lumped loads connected through seven average value model based load SSTs. The feeder is rated at 12.47 kV and is an islanded, looped system. The loads are served primarily by two diesel generators. Although the feeder is looped, it could be operated in radial mode. The two diesel generators are rated at 1.4 MVA each. One of them operates in droop mode (G2) while the other operates in isochronous mode (G1). The feeder primary is made up of seven line sections. The impedance of each line section is identical. Each load SST is rated at 285 kVA. On the secondary of each load SST, there is a lumped load, lumped distributed generation (DG) and storage connected. The generators are rated at 1.4 MVA, $380V_{L-N}$. The transformers are rated at 1.5 MVA, 0.38 kV: 12.47 kV. The transmission lines have a positive sequence resistance of 0.77 Ω, positive sequence inductance of 1.967 mH, zero sequence resistance of 2.31 Ω and a zero sequence inductance of 5.9 mH. The droop generator is set to run at 400 kW at 5% droop.

Two pairs of entities were chosen for simulation purposes. The ATC for every pair of entities were computed ahead of time. The transacting parties were made to undergo transactions in RTDS, both greater than and less than the amount that would violate the line flow invariants. Table 2.1 summarizes the nature of the cases that were considered and the results obtained.

The transactions described in Table 2.1 are not DGI enabled. These simulations were performed to test the accuracy of the line invariants before integrating them into the cyber controller. The table shows the invariant was successful in predicting transmission line overloading. The next step is to integrate the line flow invariant with DGI and perform an invariant check at every power migration level.
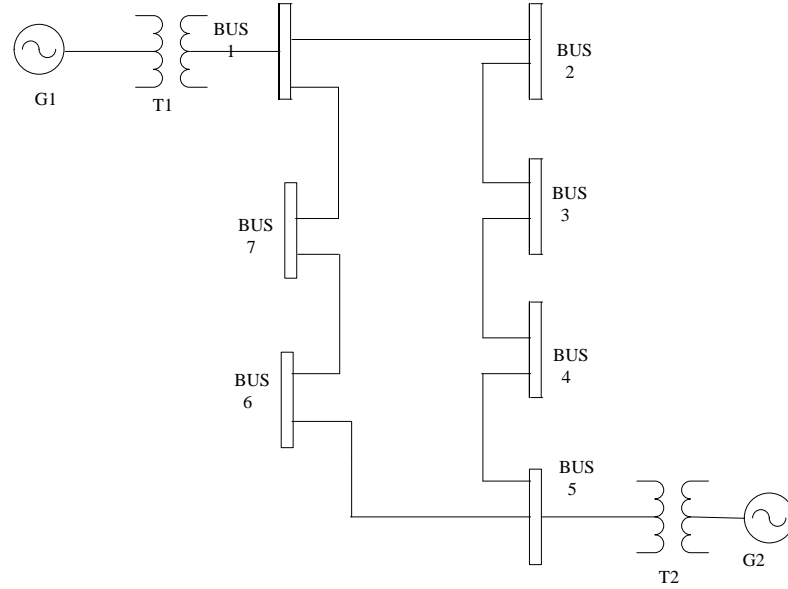
Figure 2.2. Single line diagram of the 7 bus system.

Table 2.1. Experimental table expressing the type of simulations performed.

Transacting Pairs considered	Transaction amount (MW)	ATC calculated ahead of time (MW)	Overload from simulation	Overload from invariant prediction
4 and 6	0.10	0.126	NO	NO
4 and 6	0.15	0.126	YES	YES
3 and 7	0.15	0.2	NO	NO
3 and 7	0.225	0.2	YES	YES
4 and 6; 3 and 7	0.10; 0.175	0.79; 0.141	YES	YES

2.5. LINE INVARIANT INTEGRATION WITH DGI

The RSCAD simulation was integrated with a simple distributed energy management algorithm that coordinates increases in generation and load at two buses in the system [13]. Seven processes, one for each bus in the simulation, were run across six Linux machines and made to communicate over UDP/IP sockets. Each process read its associated bus' real power injection from the simulation every 50 milliseconds. Negative real power injection values correspond to supply buses with excess generation, while positive power

injection values correspond to demand buses with excess load. The processes were also initialized with knowledge of the physical system topology which includes the location, initial real power flow, and maximum capacity of each transmission line.

The distributed energy management algorithm will pair a supply process with a demand process to perform a power transaction in the system. Unlike cases where the transactions can been defined in advance, it is impossible to control which transactions will occur when using the energy management algorithm. Therefore, PTDF values were computed for all possible pairs of one supply and one demand node in the system, and these values were stored at each of the seven processes used in the experiments. Modifications were then made to the algorithm to incorporate the invariant calculation as shown in Fig. 2.3.

Due to the distributed nature of the algorithm, there is no central controller which dictates which transactions should occur in the system. Therefore, the matrix calculation from (2.9) which was used to compute the ATC for all transacting entities by finding the base line flows, cannot be used as it is not known ahead of time which transactions will occur. Instead, an iterative approach was used in which transactions are considered to occur in a sequence where each transaction can use (2.4) to compute its ATC value. After each transaction, the base line flows, P_{ij}^0 are updated to reflect the line flow value after the most recent iteration of the algorithm. This allows (2.9) to be computed one row at a time as each iteration occurs in the distributed system.

The implementation of the invariant with the distributed energy management algorithm has been described by the flowchart shown in Fig. 2.3. The process is initialized in the second step shown on the flowchart, using a topology configuration file which includes the location, initial real power flow, and maximum capacity of each transmission line. The third step then updates the value of P_{ij}^0 for current iteration of the algorithm based on the transaction(s) that occurred in the previous iteration. After this step, the power management algorithm is unchanged from [13] until the seventh and eighth step where the invariant is
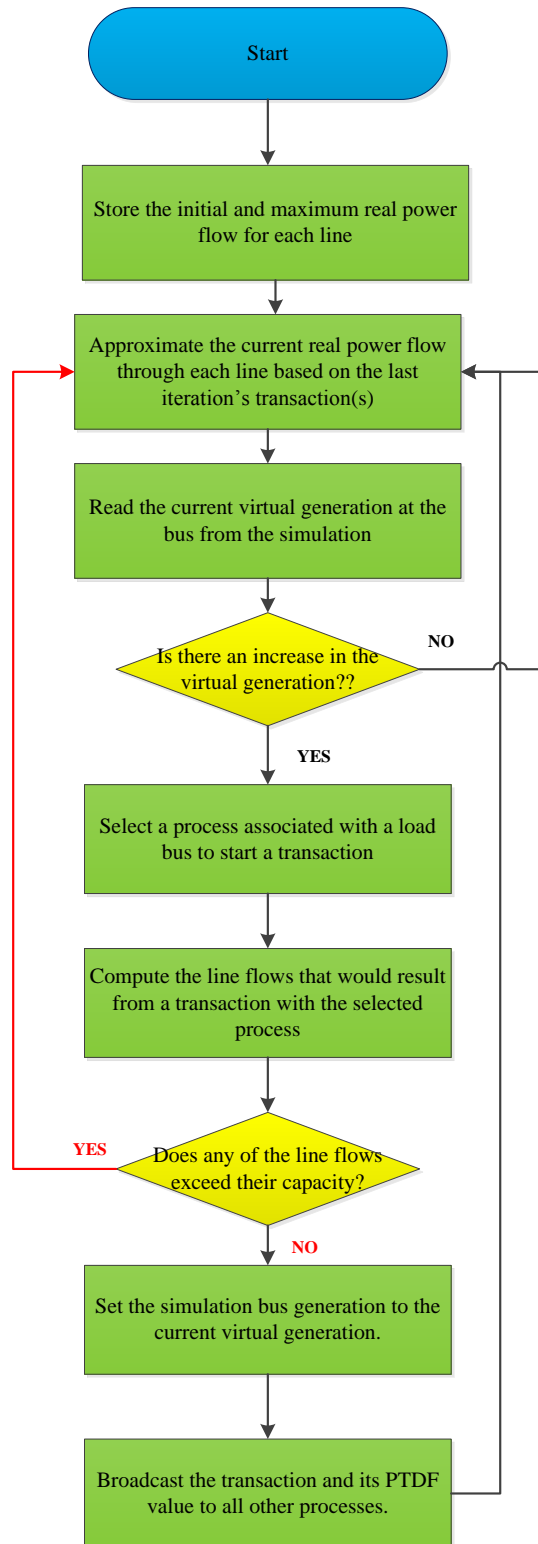
Figure 2.3. Flowchart showing distributed energy management algorithm with the invariant guard.

implemented. Step 7 uses (2.4) to compute the new line power flows that would result from the transaction selected in step 6. In effect, this predicts the effect the transaction would have on the system if it were to occur. Step 8 then compares each of these line flows to their associated maximum capacities. If any line were to exceed its capacity after the transaction, then the invariant is false and the transaction is aborted. Otherwise, the transaction is deemed safe and the energy management algorithm is allowed to continue. The last modification is at step 10, where successful transactions are broadcast to all the processes in the system to compute the line flows in the next iteration. Fig. 2.4 describes a flowchart when the invariant check is not implemented in the power management algorithm.

2.6. SIMULATION AND RESULTS

The seven node RSCAD model in Fig. 2.2 has been used to execute DGI migrations to verify the suitability of the DGI integrated line flow invariant method as described above. The seven processes were started with the RTDS simulation as described in the previous section. In the first simulation, there is a seller at sub-system 4 and a buyer at sub-system 6. For this case, the invariant check from step 8 was disabled so that processes would perform transactions regardless of the line capacities in the system. This has been illustrated in the flowchart shown in Fig. 2.4. Bus 4 was set to have 0.2 MW of maximum generation and bus 6 was set to have 0.2 MW of maximum load to allow for a potential transaction between buses 4 and 6. The ATC based line limit is 0.126 MW, calculated ahead of time, (as shown in Table 2.1) for a transaction between sub-systems 4 and 6.

The top graph in Fig. 2.5 shows the distributed energy algorithm at work, with bus 4 increasing its generation and bus 6 increasing its load in coordination with each other. Neither of these buses reach their maximum generation or load due to the design of the distributed energy management algorithm and not due to the influence of the invariant. The algorithm will only transfer fixed 0.2 MW of power. However as the DGI power migrations
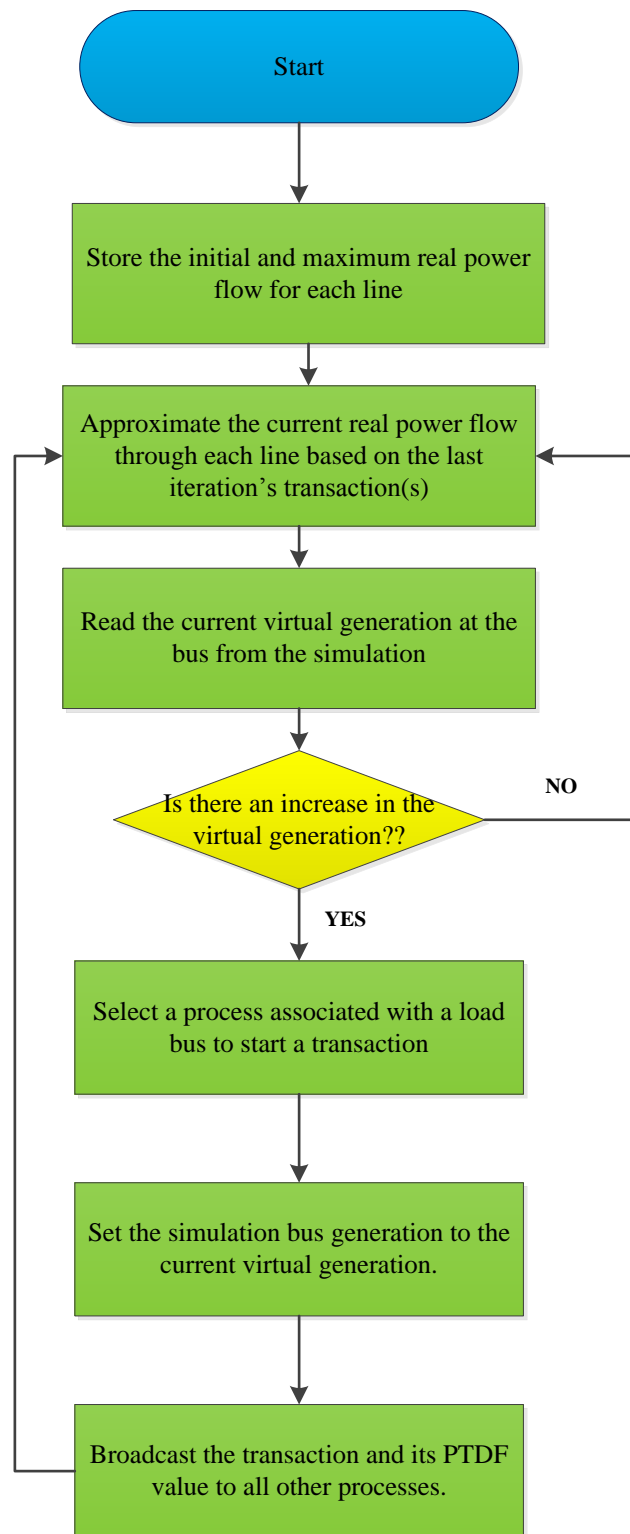
Figure 2.4. Flowchart showing the distributed energy management algorithm without the invariant guard.

increase in size, lines in the system reach their loading limits. In the absence of the invariant guard, bad transactions are permitted, resulting in consequent line overloading as shown in the middle graph of Fig. 2.5. The line flows were observed as percentage loading of their limits. The lower bottom graph in Fig. 2.5 shows the real power flow through the transmission line connecting sub-systems 5 and 6 as a percentage of its maximum loading limit. As shown, the transaction between sub-systems 4 and 6 caused this particular line to be overloaded to 1.5 times its maximum limit.
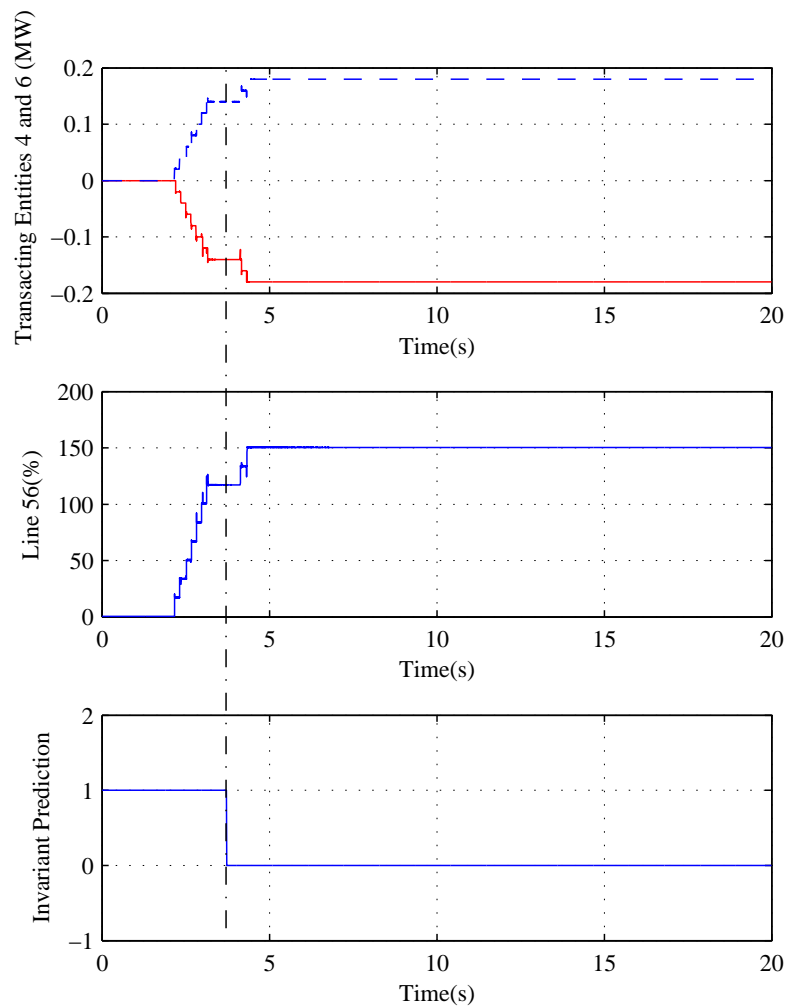
Figure 2.5. Simulated microgrid performance in response to energy management algorithm without invariant guard, indicating line overloading.

This case was then run a second time with the invariant check from step 8 in place, as described in Fig. 2.4. Fig. 2.6 shows the effect of the invariant guard on the grid behavior.

The top graph of Fig. 2.6 shows the distributed energy algorithm at work, but this time it stops far before its 0.2 MW limit. This is because of the effect of the bottom graph in Fig. 2.6 which shows the result of the invariant calculation. The middle graph shows the effect of the algorithm on the line connecting sub-systems 5 and 6.

Figure 2.6. Simulated microgrid performance in response to energy management algorithm where the invariant guards the migration, preventing line overloading.
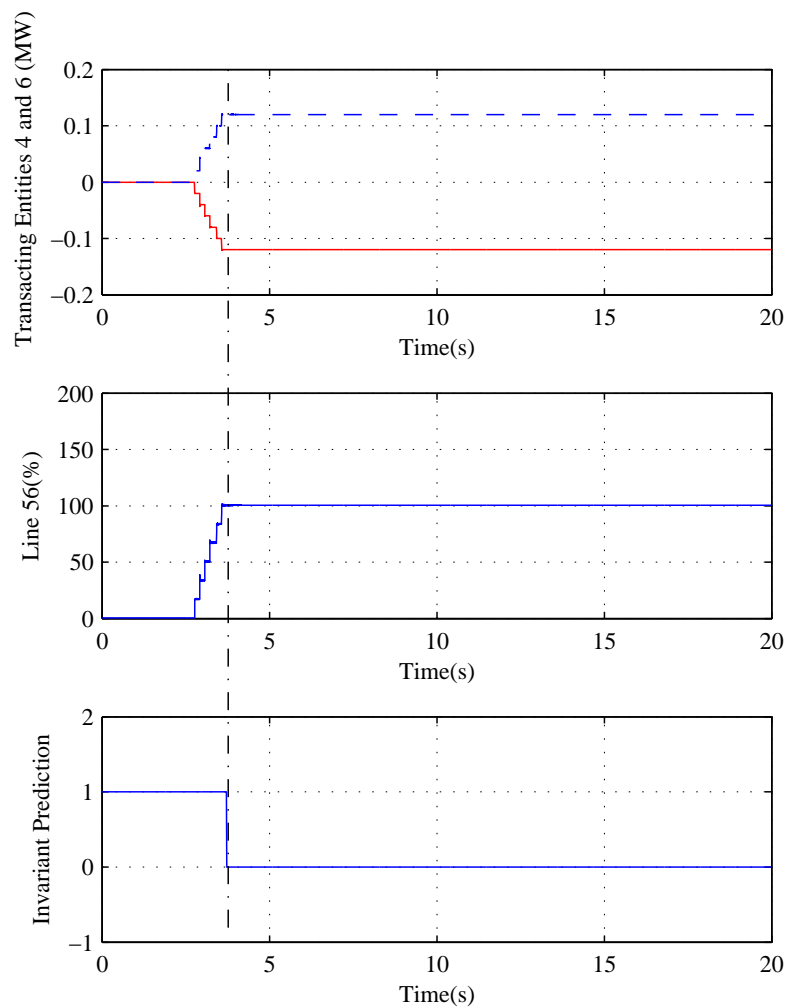
At around 4.2*s*, the algorithm determined that an additional transaction would lead to a line overload in steps 7 - 8, and refused to perform another transaction. This leads to both bus 4 and 6 stopping at real power injection values of +- 0.124 MW. Thus, the DGI enabled line invariant is intuitive enough to know that the next transaction would exceed the ATC limit (0.126 MW) for sub-systems 4 and 6. It therefore stops shortly (0.124 MW) before executing the next transaction that will cause line overloading. Only one line is loaded to its fullest extent; but not overloaded, as shown in the middle graph in Fig. 2.6. Thus unlike the previous case, this time the line does not exceed its capacity. The reason for this is because the invariant was used as a guard to protect the physical system. When the distributed algorithm determined the invariant to be false, it stopped performing transactions, and prevented the overload on this particular line.

The DGI interfaced line flow invariant was not only successful in guessing if the next transaction would overload any line in the system, but could also stop such a transaction. *Thus in a transaction based, multi party system, the DGI based method can stop any transaction that violates the line flow invariant to safeguard transmission line stability.*

2.7. CONCLUSION AND FUTURE WORK

The PTDFs have been evaluated assuming a DC load flow approach. The DC load flow method to find PTDFs is simple and less time consuming as it is a non-iterative approach. The PTDFs are used to compute the line flow invariant for any bilateral/multilateral transactions. The line flow invariant has been integrated with DGI to perform an online check on the system. If the amount prescribed by the line flow invariant is greater than the proposed transaction; only then can that particular transaction be allowed. The DGI interfaced line invariant serves not only as an important tool to test the legitimacy of a proposed transaction, but also thwart any such transaction that might cause any line to overload. This reduces the need for setting up extra transmission lines for planning new projects.

In this paper, the ATC has been computed using DCPTDFs. However ACPTDFs can also be used to compute ATC. These ACPTDFs are derived at a base case load flow result. They can be highly effective tools for computing change in any line for a change in power transactions. The ACPTDFs have the capability to evaluate the change in line flows more accurately than the DCPTDF method. Future work can be undertaken to calculate the ATC from the ACPTDFs and compare the results obtained in this paper.

The DGI-interfaced invariant based method should be extended to cases where more than one pair of sub-systems undergo transaction at the same time. The sequence of steps needed for the implementation of the algorithm in this paper assumes that each iteration performs only a single transaction. This is always the case with one pair of transacting entities, but may not be true with multiple pairs of transactions as more than one transaction could occur in the same iteration. When this happens, the approximate line flows calculated in step 3 do not account for the concurrent transactions, and thus the invariant does not correctly predict the next state of the physical system. Had either transaction occured in isolation, the invariant would not be violated, and no line overloads would have occured. However, the combination of two or more concurrent transactions may lead to a line overload, not predicted by the invariant.

There are several potential methods to tackle this problem. The easiest approach would be to allow the distributed energy management algorithm to undo its most recent action. Then in the next iteration, the algorithm could see that it violated the invariant through concurrent transactions, and each transaction from the previous iteration could be undone to limit the amount of time the lines are overloaded. An alternative and more intrusive approach would be to enforce the assumption that only a single transaction can occur per iteration. However, both of these approaches require extensive changes to the power management algorithm, and provides excellent scope for future work.

2.8. REFERENCES

[1] T. Paul, J. W. Kimball, M. Zawodniok , T. P. Roth, and B. McMillin, "Unified Invariants for Cyber-Physical Switched System Stability," *IEEE Trans. Power Syst.*, vol. 5, pp. 112–120, Jan. 2014.

[2] "Defining interconnected Operation Services Working Group", NERC, Interconnected Operation Services Working Group (IOSWG), Final Rep. 7 Mar. 1997.

[3] A. Fradi, S. Brignone, and B. F. Wollenberg, "Calculation on energy transaction allocation factors," *IEEE Trans. Power Syst.*, vol. 16, no. 2, pp. 266–272, May. 2001.

[4] Y. Ou, and C. Singh, "Assessment of available transfer capability and margins," *IEEE Trans. Power Syst.*, vol. 17, no. 2, pp. 463–468, May. 2002.

[5] R.D. Christie, B. F. Wollenberg and I. Wangensteen, "Transmission management in the deregulated environment," *Proc. IEEE*, vol. 88, no. 2, pp. 170–195, Feb. 2000.

[6] A. J. Wood, and B. F. Thompson, *Power Generation, Operation and Control*. New York: Wiley, 1996.

[7] G.C. Ejebe, J. Tong, J. Tong, J.G. Waight, X. Wang, and W.F. Tinney, "Available transfer capability calculations," *IEEE Trans. Power Syst.*, vol. 13, no. 4, pp. 1521–1527, Nov. 1998.

[8] K. Indhumathy et al, "Assessment of Available Transfer Capability (ATC) Using Linear Sensitivity Factors under Deregulated Environment," in *International Journal of Electrical Engineering and Technology*, vol. 5, no. 1, pp. 3029-3035,2013.

[9] A. Q. Huang, M. L. Crow, G. T. Heydt , J. P. Zheng, and S. J. Dale, 'The future renewable electric energy delivery and management (FREEDM) system: The energy internet," *Proc. IEEE*, vol. 99, pp. 133–148, Jan. 2011.

[10] "Calculation of available transfer capability", National programme on technology enhanced learning (NPTEL), lecture 20.

[11] Cheng. Xu, T.J. Overbye, "PTDF-based power system equivalents," *IEEE Trans. Power Syst.*, vol. 20, no. 4, pp. 1868–1876, Nov. 2005.

[12] R. Kumar, S. C. Gupta and B. Khan, "Power Transfer Distribution Factor Estimate," in *International Journal of Electrical Engineering and Technology*, vol. 2, no. 6, pp. 155-159,2013.

[13] R. Akella, F. Meng, D. Ditch , B. McMillin, and M. L. Crow, "Distributed Power Balancing for the (FREEDM) System," *First IEEE International Conference on Smart Grid Communications (SmartGridComm),* , 2010, pp. 7-12.

III. TRANSIENT STABILITY MONITORING INVARIANTS IN MICROGRIDS

Tamal Paul, Md. Rasheduzzaman, and Jonathan W. Kimball

Department of Electrical and Computer Engineering

Missouri University of Science & Technology, Rolla, MO 65409

ABSTRACT— Stability in power systems refers to the tendency of the system to return to its equilbruim position after a disturbance. The stability issue in power systems can be divided into three main categories: transient-stability, steady state stability and dynamic stability. Transient stability is the ability of the system to restore its stable configuration, even after a large disturbance. These disturbances may not cause the system to lose its synchronism, but can lead the system to a state of oscillations. If these oscillations die out quickly, the system is said to be stable. But if the oscillations continue to increase in amplitude and last for long periods of time, the system is no longer stable. Such behavior poses a serious threat to system operation and reliability. This paper attempts to preserve the transient stability of a smart grid type system with the help of invariants. An invariant is a logical predicate on a system state that must remain true throughout system execution [1]. The dynamics of a smart grid, subject to load perturbations, are modeled as a switched system. The concept of this transient stability invariant is rooted in the notion of minimum dwell time for switched systems. The invariant has been studied on a microgrid consisting of two inverters working as distributed energy resources (DER), passive loads and a distribution line. Simulation results on the microgrid have been performed to validate the invariant results.

Index Terms— dwell time, transient stability, invariant, Lyapunov, microgrid.

3.1. INTRODUCTION

Microgrids fall under a special umbrella of smart grids and are entrusted with the responsibility of improving power quality and reliability to improve system efficiency and allowing the system to operate in the absence of the grid. To quote the US Department of Energy Microgrid Exchange Group (U.S. DOE MEG) [2], a microgrid can be defined as " a group of interconneced loads and distributed energy resources with clearly defined electrical boundaries that act as a single controllable entity with respect to the grid. A microgrid can connect and disconnect from the grid to enable it to operate in both grid-connected or island mode." A smart grid forms a microgrid of distributed energy storage devices (DESDs) distributed renewable energy resources (DRERs), and LOADs (programmable and non-programmable loads) to share power for the good of the entire system. Intelligent flow controllers (Nodes) contain physical actuators such as solid state transformers (SSTs) that control power flow to and from a shared electrical bus, under direction of cooperating Distributed Grid Intelligence (DGI) Processes as shown in Fig. 3.1 [3].
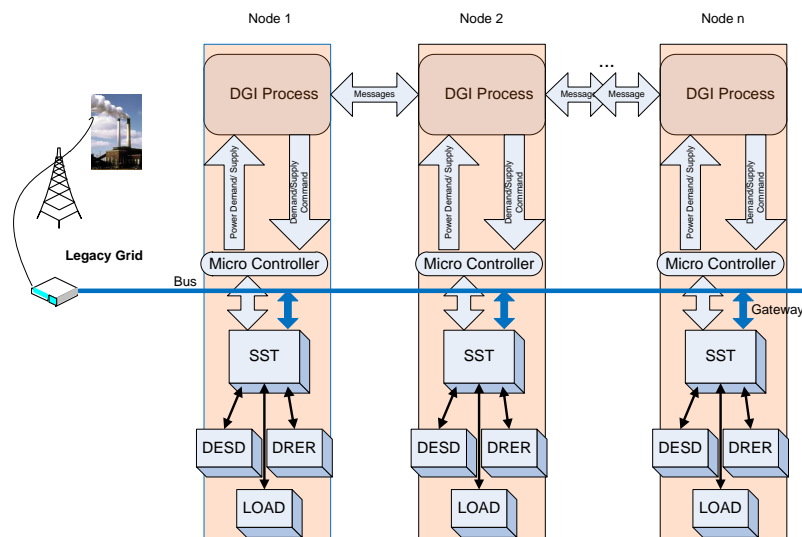

Figure 3.1. Power Management Archictecture [3].

Microgrids can operate with or without connection to the main power transmission system, i.e either islanded or grid connected. One important feature of microgrid operation is easy transitioning between these two modes [4]-[5]. When the microgrid operates in an islanded mode, its control and management becomes complex. Since in an islanded mode, the microgrid operates with finite inertia [6] (unlike infinite inertia that a grid offers), it is more prone to disturbances and stability issues. The potential for system instability is staggering: mismatch in power generation from intermittent sources such as wind and solar can cause the power grid to collapse resulting in large scale blackouts and significant equipment damage with an adverse societal influence.

There have been several attempts to study power system stability. Routh Hurwitz criterion [7], root locus techniques [8] and Nyquist method [8-11] are a few such classical methods. However all the methods described above gives a prescribed measure of stability in a given space. But this depends on the choosing the parameters of the stability zone, such that transient responses for the system is satisfactory [12]. This does not delve into the transient stability of power systems.

A microgrid, subject to load perturbations, can be modeled as a switched system. The transient stability of the microgrid can be investigated by studying the stability of switched systems.

3.2. DYNAMICS OF A SWITCHED SYSTEM

The fundamental dynamics of a switched system is that of a continuous-time system where changes occur at discrete instants of time [13]. The dynamics of a switched linear system can be given as (3.1) and (3.2) where X_σ is the steady state value at mode σ.

$$\dot{\tilde{x}} = A_\sigma \tilde{x} \tag{3.1}$$

$$x = \tilde{x} + X_\sigma \tag{3.2}$$

When the mode is switched from i to j, the new dynamics are given by (3.3) where $\Delta_j = x_j$-x_i. $\dot{\tilde{x}} = A_\sigma \tilde{x}$ is the linearization of $\dot{X} = f_\sigma(X)$ around X_σ where X_σ is a stable point.

$$x(t_j^+) = \tilde{x}(t_j) + \Delta_j \tag{3.3}$$

For such a system to be asymptotically stable, all the eigenvalues of the A_σ matrix must have real negative parts [13]. The Lyapunov function for such a system can be found by fixing an arbritary positive definite symmetric matrix Q and finding an unique positive definite symmetric matrix P that satisfies the Lyapunov equation

$$A^T P + PA = -Q \tag{3.4}$$

Solving this equation , it is possible to obtain the Lyapunov function $V(\tilde{x}) = \tilde{x}^T P \tilde{x}$ which gives a derivative of

$$\dot{V} = -\tilde{x}^T Q \tilde{x} \tag{3.5}$$

Thus, the system is asymptotically stable if and only if P and Q satisfy (3.4). However, when the system is switching, asymptotic stability of each node is not sufficent to ensure the stability of the entire system.

3.3. INVARIANTS FOR TRANSIENT STABILITY IN POWER SYSTEMS

Lyapunov functions can be used to study complex systems such as the power grid [1]. Lyapunov functions must be positive definite, radially unbounded and non increasing for the system to be stable. This can be represented as the following set of equations.

$$V(x) > 0 \ \forall \, x \neq 0 \tag{3.6}$$

$$V(0) = 0 \tag{3.7}$$

$$\frac{dV}{dt} \leq 0 \tag{3.8}$$

If $\frac{dV}{dt}$ is non-positive, the system is stable. If $\frac{dV}{dt}$ is strictly negative, the system is asymptotically stable [1].

For a switched system with different operating modes, multiple Lyapunov functions can be considered. A system operating in two modes (say) can have two Lyapunov functions, V_1 and V_2, describing the dynamics of each mode. Each of these modes can be stable independently. However when the system is switched in between these modes, it is possible to drive the system to instability by controlling the time in between switching. This introduces us to the notion of *dwell time* will be explained later in this section. The stability of such a switched system, having otherwise stable operating modes (described by Lyapunov functions) can be analyzed with the help of another set of functions known as Lyapunov-like functions [14-16]. Lyapunov like functions should also be positive definite and radially unbounded just like their Lyapunov counterparts. However, the derivative does not need to be negative at all times. For such class of functions, the value of the function at the switching instants is what matters.

A switched system operating in multiple modes, enumerated by i can be considered. A Lyapunov like function can be composed for each operating mode. However if the system is switching between various modes, the only values of $V_i(x_i)$ that are of relevance are the values at the instants when switching occurs. If those values show a non increasing or decreasing trend for all switching modes and all admissible values of i, then the switched
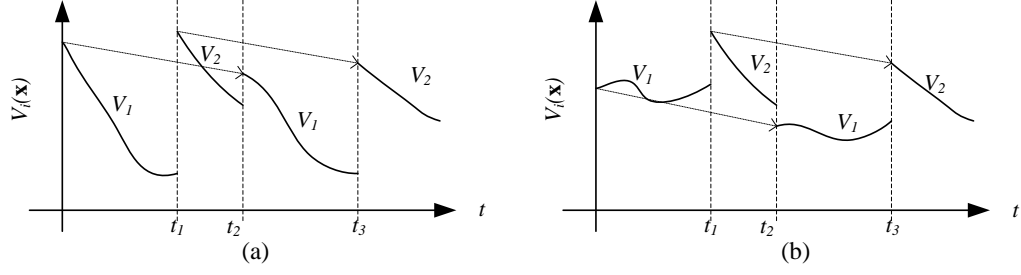
Figure 3.2. Switched system stability using multiple Lyapunov functions (V_1 and V_2) [1].

system is stable. This concept had been shown in Fig. 3.2. Fig. 3.2(a) shows true Lyapunov functions for both modes, and the times at which they switch follow a decreasing pattern thereby indicating system stability. Fig. 3.2(b) shows at least one mode cannot be described by a true Lyapunov function. However, the overall system is stable, because V_1 and V_2 have a decreasing trend.

A switched system is stable if all the operating modes are stable and the switching times are long enough to ensure that the transients of the previous mode had settled down before the next mode is switched on. This again brings back the time concept in between switching. For switched systems, a number τ_d can be assigned [13] such that switching times in between the modes should always be greater than that number, to ensure system stability. This number τ_d is called dwell time. This nomenclature may be attributed to the fact that the switched system needs to "dwell" in each mode for at least τ_d amount of time [13].

If the individual operating modes are asymptotically stable, the switched system is also asymptotically stable if the switching time in between the modes are greater than the dwell time. A lower bound on the dwell time can be derived from the exponential decay bounds on the state transition matrices of the individual operating modes [13]. For a system with stable operating modes, Lyapunov functions (V_i) for each mode satisfy (3.9) and (3.10) for some positive values of a_i, b_i and c_i [13].

$$a_i \, | \, x \, |^2 \leq V_i(x) \leq b_i \, | \, x \, |^2 \qquad (3.9)$$

$$\dot{V}(x) \leq -c_i \, | \, x \, |^2 \qquad (3.10)$$

(3.9) and (3.10) can be combined to obtain (3.11) where $k_i = \frac{c_i}{2b_i}$.

$$\dot{V}(x) \leq -2k_i V_i(x) \qquad (3.11)$$

A lower bound on the dwell time can be derived which ensures that the switched system is asymptotically stable. For a system operating between two modes, a generalized expression of this dwell time can be given by (3.12) [13].

$$\tau_d = \frac{1}{2(k_1 + k_2)} log \frac{b_1 b_2}{a_1 a_2} \qquad (3.12)$$

The concept of dwell time can be used to formulate invariants for preserving the transient stability of power systems. Power systems can be modeled as switched systems, as load perturbations can act as different operating modes. For a power system operating back and forth between different operating modes (change in load patterns), the notion of dwell time can be extended to describe the stability of the system. The invariant to preserve transient stability can be expressed as : *The system is stable if the switching time in between the operating modes is greater than the minimum dwell time derived for the system.* It is possible to even drive a system with stable operating modes to instability by violating the minimum dwell time requirement for the system.

3.4. SIMULATION AND RESULTS

The microgrid system adopted for this study has been shown in Fig. 3.3. The inverters are connected to their respective buses by a filter. The variable passive loads connected to these buses serve as local loads. The microgrid is operating in islanded mode. A small signal model of this system was developed in PLECS[®][2]. Details about the development of the this small signal inverter dominated microgrid model has been described in [17].
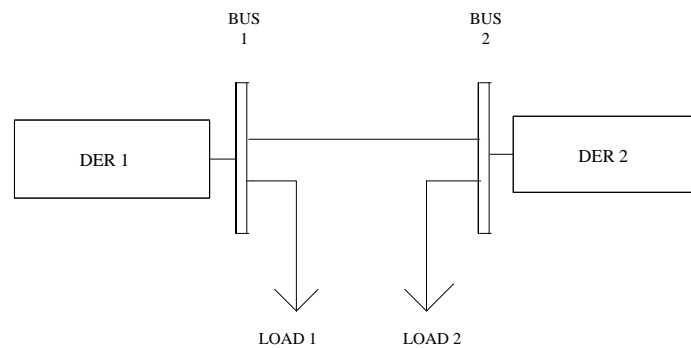

Figure 3.3. Microgrid model for stability studies [17].

Singular perturbation methods [18-19] have be used to reduce the full order model to a reduced order model by removing the fast dynamic states without losing the physical nature of the states [17]. A model order reduction algorithm has been used to reduce the order of the islanded system. The reduced order system has only 15 differential equations as compared to 36 differential equations in the full order system. The reduced order model is then linearized around stable operating points. This is done by simulating an average value model of the system described in the figure above in PLECS[®].

The loads are connected to the inverter buses. The load resistances are in the order of 25Ω. At the start of the simulation, load 'a' is connected to bus 1 and bus 2. This is our

---

[2]PLECS[®] is a registered trademark of Plexim GmbH

first operating mode. A set of operating points corresponding to this mode is given by X_1. After a certain amount of time t_{sw}, load 'b' (also 25Ω) is connected in parallel to the initial load at bus 1 to mimic a change in loading condition. This gives a second set of operating points for a second operating mode. The second set of operating points are given by X_2. The detailed value of the entries in the matrices X_1 and X_2 have been presented in [17]. The system state transition matrices for these two modes, A_1 and A_2 are obtained through linearization around stable operating points given by X_1 and X_2.

The two inverter model can thus be made to switch back and forth between two operating modes by switching the load 'b' at bus 1 ON and OFF and controlling the switching times. If the modes are enumerated by i, and their respective Lyapunov-like functions as $V_k(x_k)$, then the Lyapunov-like functions for modes 1 and 2 can be represented as $V_1(x_1)$ and $V_2(x_2)$. The Lyapunov functions for the two modes can be expressed as :

$$V_1(x_1) = x_1^T P_1 x_1 \qquad\qquad (3.13)$$

$$V_2(x_2) = x_2^T P_2 x_2 \qquad\qquad (3.14)$$

The P matrices that satisfy (3.13) and (3.14) must be positive definite, for the switched system to be stable. The dwell time can be calculated from (3.12). For a linear system, the upper and lower bounds on the Lyapunov function from (3.9) for a certain mode are given by the maximum and minimum eigen values for the P matrix of that operating mode. The upper bound in (3.10) is given by the maximum eigen value of the Q matrix of that operating mode. Using the maximum and minimum eigen values for P_1 and P_2, a_1, b_1, a_2 and b_2 were evaluated. The maximum eigen values for Q_1 and Q_2 yielded values for c_1 and c_2. Using (3.11) and (3.12), the dwell time was computed to be $1.933s$ for the model used in this paper. For the experiment reported in this paper, the dwell time was chosen such that it is greater than $1.933s$.

The system is in its initial mode, Mode 1, for the first $1s$ when load 'b' at bus 1 is OFF. Load 'b' is switched ON after $1s$ thereby transitioning from Mode 1 to Mode 2 . At $t = 3.0s$, load 'b' is switched OFF; thereby reverting back to Mode 1. At again $t = 5.0s$, load 'b' is switched ON and the system is back in Mode 2. Load 'b' is again switched OFF at $t = 7.0s$, thereby bringing the system back to Mode 1. The swtiching modes are represented by the top graph in Fig. 3.4. where the switching mode values represent the current operating mode of the system. For the operating points X_1 and X_2, corresponding to Modes 1 and 2, the system state is described by the matrices A_1 and A_2. The dwell time in this case is thus $2.0s$, which does not violate the minimum dwell time based transient stability invariant.

The multiple Lyapunov-like functions for this switched system can be plotted against time as shown in the bottom graph in Fig. 3.4. The P matrices for each mode were found to be positive definite.
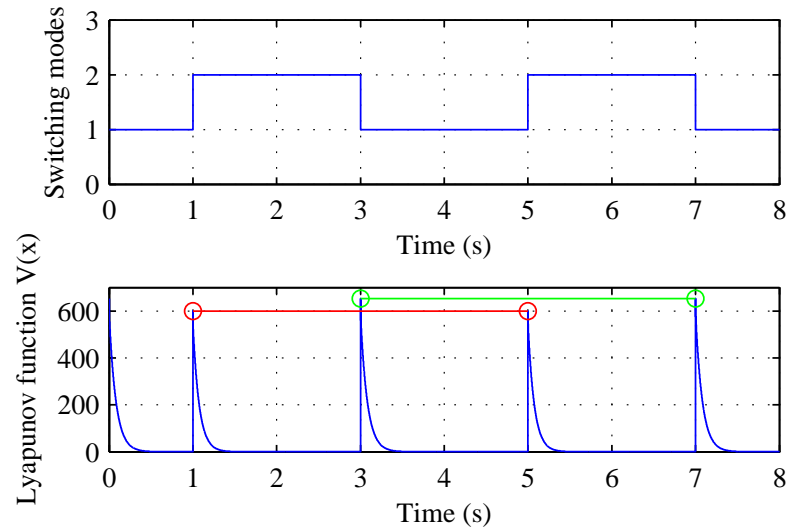

Figure 3.4. Switched sequence of the microgrid model showing Lyapunov-like stability, as depicted by the non increasing trendlines at the switching instants.

The graph at the bottom of Fig. 3.4 plots the Lyapunov-like function for the given system. Every time there is a mode change, the function increases. However, after the

initial increase, the function peaks and then there is a strict monotonic decrease at the beginning of each mode. This implies that the system is stable, and the steady-state behavior can be studied at the end of switching. This behavior is depicted by circles on the trendlines and correspond to changes in operating modes due to the ON/OFF action of load 'b' at bus 1. There are two trendlines depicted in the graph, one red and one green. The red trendlines denote the switching of the system from Mode 1 to Mode 2 and the green trendline denotes the switching of the system from Mode 2 to Mode 1. Both these trendlines are non increasing which satisfies the transient stability invariant. Fig. 3.5 shows the transient response of the system in terms of active and reactive power, which iterates the system stability denoted by the Lyapunov-like functions.

The Lyapunov-like stability of the system has been compared with simulation results as shown in Fig. 3.5. The load changes occur at $1s$, $3s$, $5s$ and $7s$. The active and reactive power of both the inverters have been plotted, using solid red lines for inverter 1 and dashed blue lines for inverter 2. Despite all the load changes, the transient response of the system is shown to settle down. When the minimum dwell time invariant is satisfied, the transient response of the system validated that system stability was maintained. Thus if the dwell time is sufficiently high, the states can go back to their equilibrium position and the overall system will be stable. However if the states are not given enough time to settle down before the next mode is switched on, the system can go unstable. Thus switching too soon, or "too much" switching action can reduce the dwell time needed for stability. This reduced dwell time will interfere with the system dynamics. As a result, the system function will cease to be Lyapunov-like and this should also be reflected in the transient response of the system. Such an unstable case, generated by switching the system too quickly can be achieved by violating the minimum dwell time based transient stability invariant.

Conceptually if the dwell times between the operating modes are reduced to less than $1.933s$, the system may be unstable. However, it has not been possible to simulate such an unstable case for this model. This is due to the extremely loose bound on the
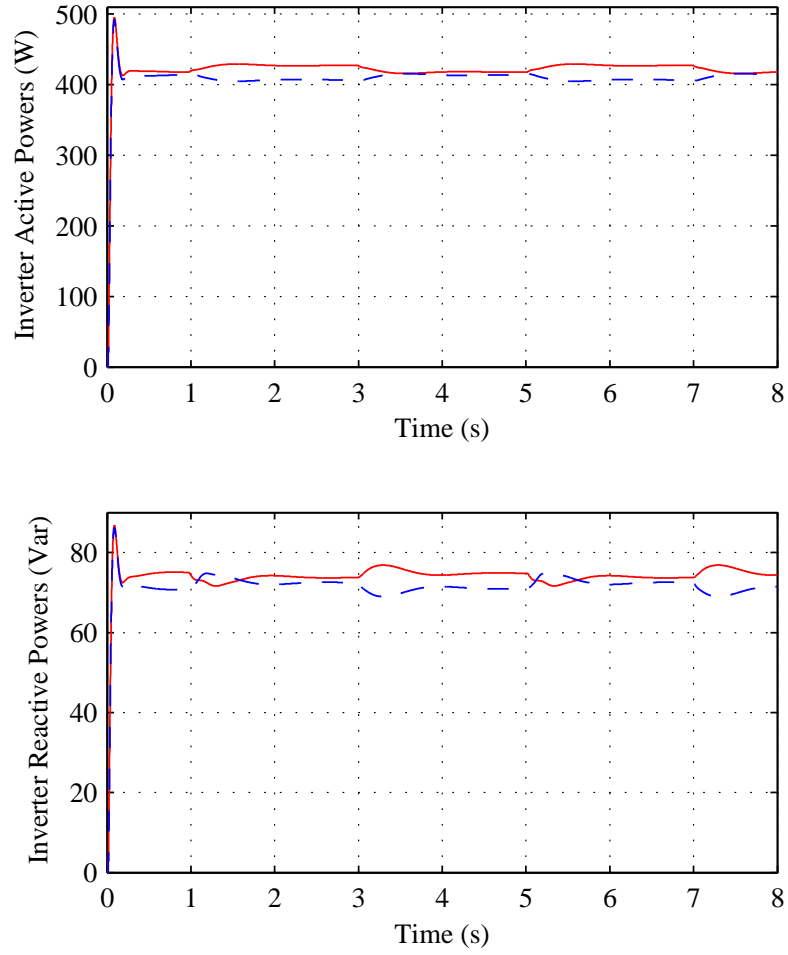
Figure 3.5. Inverter active and reactive power outputs in response to microgrid switching.

minimum dwell time computed for this model. This loose bound can be explained by the nature of the P matrices. In order for a tight lower bound on dwell time, the maximum and minimum eigenvalues of the P matrices should be in a comparable range. However, for P_1, the maximum and minimum eigenvalues are 0.22291 and 7.042e-10; for P_2, the maximum and minimum eigenvalues are 0.22435 and 6.987e-10. This extreme difference in the range of maximum and minimum eigenvalues contributes to the extremely loose bound on the dwell time.

3.5. CONCLUSION

This paper presents a transient stability invariant to monitor the transient stability in smart grid type applications, subject to load perturbations. The load perturbations are analogous to switching actions. Switched system stability concepts have thus been extended to study the transient stability of a microgrid. The stable Lyapunov-like behavior of the two-inverter microgrid model, when subjected to load perturbations have been validated by the transient response of the active and reactive powers of both the inverters. Similar power system applications can be modeled as switched autonomous systems [17].

The maximum and minimum eigenvallues of the P matrices should be in a comparable range to obtain a stricter bound on the dwell time if the system is to be driven to instability. The invariant presented in this paper is extremely loose and the system stability is not at all perturbed when the invariant is violated. Better bounds should be found for the minimum dwell time to observe an unstable case on violating the invariant. In addition to this Lyapunov based method of stability, Markov Jump Linear Systems (MJLS) can also be used to study power system dynamics. A MJLS is a dynamic system with continuous states and a continuous time Markov process. There is a jump in the continuous state dynamics of the system when the discrete state of the Markov process changes [20]. After investigating the effects of deterministic switching, it can be possible to employ the concept of MJLS to study random switching in the context of microgrids.

3.6. REFERENCES

[1] T. Paul, J. W. Kimball, M. Zawodniok , T. P. Roth, and B. McMillin, "Unified Invariants for Cyber-Physical Switched System Stability," *IEEE Trans. Power Syst.*, vol. 5, pp. 112–120, Jan. 2014.

[2] M. Smith and D. Ton, "Key connections: The U.S. department of energy's microgrid initiative," *IEEE Power and Energy Magazine*, vol. 11, no. 4, pp. 22–27, Jul. 2013.

[3] A. Q. Huang, M. L. Crow, G. T. Heydt , J. P. Zheng, and S. J. Dale, 'The future renewable electric energy delivery and management (FREEDM) system: The energy internet," *Proc. IEEE*, vol. 99, pp. 133–148, Jan. 2011.

[4] A. L. Dimeas, and N.D Hatziargyriou, "Operation of a multiagent system for microgrid control," *IEEE Trans. Power Syst.*, vol. 20, no. 3 pp. 1447–1455, Aug. 2005.

[5] J. A. P Lopez, C. L. Moreira, and A.G Madureira, "Defining control strategies for microgrid ESS islanded operation," *IEEE Trans. Power Syst.*, vol. 21, no. 2 pp. 916–924, May 2006.

[6] H. Nikkhajoei, and R. H. Lasseter, "Distributed generation interface to the CERTS microgrid," *IEEE Trans. Power Del.*, vol. 24, no. 3 pp. 1598–1608, Jul. 2009.

[7] Y. N. Yu, and K. Vongsuriya, "Steady-state stability limits of a regulated synchronous machine conected to an infinite system," *IEEE Trans. Power Apparatus and Systems*, vol. PAS-85, no. 7 pp. 759–767, Jul. 1996.

[8] C. A. Stapleton, "Root-locus study of synchronous machine regulation," *Proc. IEEE*, vol. III, no. 4, pp. 761–768, April 1964.

[9] H. K. Messerle and R. W. Bruck, "Steady-state stability of synchronous generators as affected by regulators and governors," *Proc. IEEE*, Part c, vol. 102, pp. 24–34, 1955.

[10] L. J. Jacovides and B. Adkins, "Effect of excitation regulation on synchronous-machine stability," *Proc. IEEE*, vol. 113, no. 6, pp. 1021–1034, June 1966.

[11] A. S. Aldred and G. Shackshaft, "A frequency- response method for the predetermination of syn- chronous-machine stability," *Proc. IEEE*, vol. 107c, pp. 2–10, 1960.

[12] M. M. Elmetwally and N. Dharma Rao, "Sensitivity Analysis in Power System Dynamic Stability Studies," *IEEE Trans. Power Apparatus and Systems*, vol. PAS-91, no. 4, pp. 1692 – 1699, July/Aug. 1972.

[13] D. Liberzon, *Switching in Systems and Control*. Boston: Birkhauser, 2003.

[14] M. S. Branicky, "Multiple Lyapunov functions and other analysis tools for switched and hybrid systems," *IEEE Trans. Autom. Control*, vol. 43, no. 4, pp. 475–482, 1998.

[15] H. Ye, A. N. Michel, and L. Hou, "Stability analysis of systems with impulse effects," *IEEE Trans. Autom. Control*, vol. 43, no. 12, pp. 1719–1723, 1998.

[16] H. Ye, A. N. Michel, and L. Hou, "Stability theory for hybrid dynamical systems," *IEEE Trans. Autom. Control*, vol. 43, no. 4, pp. 461–474, 1998.

[17] Md. Rasheduzzaman, J. A. Mueller, J. W. Kimball, "An Accurate Small-Signal Model of Inverter-Dominated Islanded Microgrids using *dq* Reference Frame," *IEEE Journal on Emerging and Selected Topics in Power Electronics*, vol. 2, no. 4, pp. 1070-1080, Dec. 2014.

[18] P. V. Kokotovic, H. K. Khali, and J. O'Reilly, *Singular Perturbation Methods in Control: Analysis and Design*, ser. TJ213.K3924, 1999.

[19] D. Naidu, *Singular Perturbation Methodology in Control Systems*, Dec. 1987.

[20] M. Rasheduzzaman, T. Paul, and J. W. Kimball, "Markov jump linear system analysis of microgrid," in *Proc. of American Control Conf. (ACC) 2014*.

SECTION

2. CONCLUSION AND FUTURE WORK

The focus of this research has been to combine the diverse environments of physical systems, computer networks and communications in a common semantic. Unified Invariants approach has been adopted to compose safe, stable cyber-physical systems. The key has been to ensure non-interference of actions. Non-interference of actions suggest that actions in a particular domain should not interfere with the functioning of another domain. For instance, a cyber message or a network delay should not violate the physical invariant. It has been established that invariants are a natural solution to tackle the CPS research problem. Unified invariants tie all the domains of a CPS and non interference is the glue that holds them together. Various invariants have been developed in this dissertation to maintain system correctness. This correctness can be quantified in terms of voltage stability, line loading or transient stability. These physical invariants have been validated on a smart grid type system.

Future work will be to integrate these physical invariants with cyber invariants and network invariants, so as come up with an overall system invariant. These integrated invariants will guard an adaptive real time environment to ensure that the system is operating correctly even in the presence of adversities such as errors introduced by codes that are not type safe, lack of information, decentralized and degraded operating conditions.

VITA

Tamal Paul received his B.Tech degree in Electrical Engineering from National Institute of Technology Durgapur, India in 2010, and his M.S. degree in Electrical Engineering from the Missouri University of Science and Technology (Missouri ST), Rolla, MO, USA, in 2012 where he is currently working towards his Ph.D degree. His current research interests include analysis, design, and control of switched system stability in cyber-physical systems.